Y 3.N 88:25/
0169/v.10

US GOVERNMENT PUBLICATIONS (depository)
Nuclear Regulatory Coms
LOFT experimental measurements...analyses 1981-

Mar 83-8256
1 of 1
p.0001-0057

READEX

1051-H-11
Y3.N88:25/0169/V.10

NUREG/CR-0169
EGG-2037
Vol. X

COMPLETED
69
ORIGINAL

U.S. Department of Energy
Idaho Operations Office • Idaho National Engineering Laboratory

LOFT Experimental Measurements Uncertainty Analyses Volume X Absolute Pressure Measurement Uncertainty Analysis

Scott Ploger

September 1981

Prepared for the
U.S. Nuclear Regulatory Commission
Under DOE Contract No. DE-AC07-76IDO1570

EG&G Idaho

NOTICE

This report was prepared as an account of work sponsored by an agency of the United States Government. Neither the United States Government nor any agency thereof, nor any of their employees, makes any warranty, expressed or implied, or assumes any legal liability or responsibility for any third party's use, or the results of such use, of any information, apparatus, product or process disclosed in this report, or represents that its use by such third party would not infringe privately owned rights.

Available from

GPO Sales Program
Division of Technical Information and Document Control
U.S. Nuclear Regulatory Commission
Washington, D.C. 20555

and

National Technical Information Service
Springfield, Virginia 22161

NUREG/CR-0169
EGG-2037
Vol. X
Distribution Category: R2

LOFT EXPERIMENTAL MEASUREMENTS UNCERTAINTY ANALYSES VOLUME X ABSOLUTE PRESSURE MEASUREMENT UNCERTAINTY ANALYSIS

Scott Ploger

Published September 1981

EG&G Idaho Inc.
Idaho Falls, Idaho 83415

Prepared for the
U.S. Nuclear Regulatory Commission
Washington, D.C. 20555
Under DOE Contract No. DE-AC07-76IDO1570
FIN No. A6043

III

ABSTRACT

A measurement uncertainty and response time analysis is presented for the five types of experimental absolute pressure transducers currently installed on the Loss-of-Fluid Test (LOFT) reactor. Specific sources of measurement uncertainty and response lag are described, quantified, combined, and compared to requirements in order to provide an overall assessment of absolute pressure measurement system performance. The measurement uncertainties were found to be within the tolerances specified in the system requirements documentation when recorded in parallel on one digital and one analog system.

SUMMARY

Absolute pressure measurement uncertainties from calibration, thermal shifts, adjustments to absolute pressure, and from data recording have been estimated. These uncertainties have been combined into total zero-offset (bias) and total pressure-dependent values at the 95% confidence level for each type of experimental absolute pressure measurement made on the Loss-of-Fluid Test (LOFT) reactor. These uncertainty values are summerized in the table below.

	Primary Coolant System			Blowdown Suppression System	
Uncertainty	Reference[a] (17.24 MPa)[b]	Wide Range (20.69 MPa)	Narrow Range (1.38 MPa)	(0.69 MPa)	(3.48 MPa)
Bias Uncertainty B (in MPa)					
Digital Recording	$\pm 4.3 \times 10^{-2}$	$\pm 7.7 \times 10^{-2}$	$\pm 4.8 \times 10^{-2}$	$\pm 1.3 \times 10^{-2}$	$\pm 1.2 \times 10^{-2}$
Analog Recording	±0.20	±0.24	$\pm 5.0 \times 10^{-2}$	$\pm 1.5 \times 10^{-2}$	$\pm 4.1 \times 10^{-2}$
Percent of Pressure Uncertainty RD (no units)	±0.30	±0.57	±0.44	±0.47	±0.20

a. Transducer type.

b. Transducer range.

For any of the five transducer types, the uncertainty U is calculated by first multiplying the pressure-dependent, percent of reading uncertainty RD (dimensionless) by the pressure reading P (MPa). The result is divided by 100, and the divided value is finally added to the bias uncertainty B (in MPa) that is appropriate to the recording medium used. Equivalently,

$$U \text{ (95\% confidence)} = \pm \left(B + \frac{P \cdot RD}{100} \right).$$

Response times (10 to 90%) have been estimated for the pressure transducers, pressure transmission tubes, electronic filters, and for the data recording systems. The combined results of these calculations are:

	Digital Recording, Small-Break Transient	Digital Recording, Large-Break Transient	Analog Recording
Primary Coolant System	0.365 s	6.25×10^{-2} s	1.34×10^{-2} s
Blowdown Suppression System	0.352 s	4.97×10^{-2} s	7.83×10^{-4} s

Comparisons have been made between the above estimated performance levels and applicable absolute pressure measurement requirements established by the LOFT Program. The LOFT absolute pressure measurements meet the accuracy requirements, with the exceptions of the blowdown-suppression-system measurements at particularly low pressures, when the data are recorded digitally. The LOFT measurements surpass the response requirements when analog recording is used. All requirements are met when the data are recorded in parallel on one digital and one analog system. It follows that the recording systems currently available are the limiting factors in overall measurement system performance.

FOREWORD

This document (NUREG/CR-0169, EGG-2037, Volume X[a]) is one of a series of reports on uncertainty analyses for measurement systems used in the Loss-of-Fluid Test (LOFT) program. Measurement uncertainty analyses are performed to evaluate the anticipated performance uncertainty for each experimental measurement in the LOFT system. Results of these analyses are reported in a series of volumes designated NUREG/CR-0169, EGG-2037. Volume I of this series will describe the LOFT experimental measurement system and the technique used for calculating the uncertainties. The remaining volumes in the series will present detailed results from the uncertainty analysis performed for each experimental measurement system.

The following volumes have preceded Volume X:

1. P. A. Quinn, G. L. Biladeau, R. Y. Maughan, *LOFT Experimental Measurements Uncertainty Analyses, Volume V, LOFT External Accelerometer Uncertainty Analysis*, NUREG/CR-0169, TREE-1089, October 1978.

2. G. L. Biladeau, *LOFT Experimental Measurements Uncertainty Analyses, Volume VI, LOFT Linear Variable Differential Transformer Displacement Transducer Uncertainty Analysis*, TREE-NUREG-1089, February 1978.

3. G. D. Lassahn, *LOFT Experimental Measurements Uncertainty Analyses, Volume VII, LOFT Self-Powered Neutron Detector Uncertainty Analysis*, NUREG/CR-0169, TREE-1089, August 1978.

4. G. D. Lassahn and P. A. Quinn, *LOFT Experimental Measurements Uncertainty Analyses, Volume VIII, LOFT Traversing In-Core Probe Uncertainty Analysis*, NUREG/CR-0169, TREE-1089, August 1978.

5. G. L. Biladeau, *LOFT Experimental Measurements Uncertainty Analyses, Volume IX, LOFT Strain Gage Uncertainty Analysis*, TREE-NUREG-1089, June 1978.

6. S. Silverman, *LOFT Experimental Measurements Uncertainty Analyses, Volume XIV, LOFT Drag Disc-Turbine Transducer Uncertainty Analysis*, NUREG/CR-0169, TREE-1089, November 1978.

7. L. D. Goodrich, *LOFT Experimental Measurements Uncertainty Analyses, Volume XV, LOFT Primary Coolant Pump Speed Measurement Uncertainty Analysis*, TREE-NUREG-1089, April 1978.

8. G. D. Lassahn, *LOFT Experimental Measurements Uncertainties Analyses, Volume XVI, LOFT Three-Beam Gamma Densitometer System*, TREE-NUREG-1089, February 1978.

9. G. D. Lassahn, *LOFT Experimental Measurements Uncertainty Analyses, Volume XVIII, Radiation-Hardened Gamma Densitometer*, NUREG/CR-0169, EGG-2037, September 1980.

---

a. Volumes VI, IX, XV, and XVI were published prior to implementation of the NUREG/CR numbering system as TREE-NUREG-1089; Volumes V, VII, VIII, and XIV were published as NUREG/CR-0169, TREE-1089 (TREE was the former designation for formal reports prepared by EG&G Idaho, Inc.). The remaining volumes in this series of uncertainty analyses will be published as NUREG/CR-0169, EGG-2037.

ACKNOWLEDGMENTS

The author extends his thanks to R. J. Boring and G. G. Neff for obtaining hardware and procedural information, and to G. D. Lassahn and L. D. Goodrich for technical assistance in the writing and reviewing of this report.

CONTENTS

ABSTRACT ii

SUMMARY iii

FOREWORD v

ACKNOWLEDGMENTS vi

1. INTRODUCTION 1

1.1 Absolute Pressure Measurement Applications 1

1.1.1 Reactor-Vessel Measurements 2
1.1.2 Primary-Coolant-Piping-System Measurements 2
1.1.3 Blowdown-Suppression-System Measurements 3

1.2 Absolute Pressure Measurement Requirements 3

1.2.1 Accuracy 3
1.2.2 Response 3

2. DESCRIPTION 5

2.1 Transducer Hardware 5

2.2 Transducer Installation 7

2.2.1 Primary Coolant System 7
2.2.2 Blowdown Suppression System 13

2.3 Measurement System Electronics 13

3. REFERENCE MEASUREMENTS 15

3.1 Calibration and Traceability Uncertainties 15

3.2 Thermal Variations 16

3.3 Absolute Pressure Adjustment 16

3.4 Data Recording Errors 17

3.5 Reference Measurement Summary 17

4. WIDE-RANGE MEASUREMENTS 18

4.1 Calibration Coefficient Uncertainties 18

4.1.1 The K Factor 19
4.1.2 The C Factor 19
4.1.3 The B Factor 20
4.1.4 The S Factor 20
4.1.5 Calibration Uncertainty Summary 21

4.2 Data Recording Errors 23

4.3 Transducer Height Differences 23

4.4 Wide-Range Measurement Summary 24

5. NARROW-RANGE MEASUREMENTS 25

5.1 Zero-Offset Uncertainties 25

5.1.1 Calibration Uncertainty 25
5.1.2 Transducer Temperature Variations 26
5.1.3 Data Recording Errors 26

5.2 Pressure-Dependent Uncertainties 26

5.2.1 Transducer Response Variations 27
5.2.2 Transducer Temperature Variations 27

5.3 Narrow-Range Measurement Summary 27

6. BLOWDOWN-SUPPRESSION-SYSTEM MEASUREMENTS 28

6.1 Zero-Offset Uncertainties 28

6.1.1 Calibration Uncertainties 28
6.1.2 Transducer Temperature Variations 28
6.1.3 Absolute Pressure Adjustment 29
6.1.4 Data Recording Errors 29

6.2 Pressure-Dependent Uncertainties 29

6.2.1 Transducer Response Variations 29
6.2.2 Transducer Temperature Variations 29

6.3 Suppression-System Measurement Summary 30

6.3.1 Zero-Offset Uncertainties 30
6.3.2 Pressure-Dependent Uncertainties 30

7. RESPONSE LIMITATIONS 31

7.1 Standoff Tube Delays 31

7.2 Standoff Tube Resonances 32

7.3 Transducer Response 34

7.4 Data System Response 34

7.5 Response Limitation Summary 34

8. CONCLUSIONS 36

8.1 Measurement Accuracy 36

8.2 Measurement Response 36

8.3 Measurement Performance Overview 38

9. REFERENCES 39

APPENDIX A—PRESSURE TRANSDUCER PERFORMANCE SPECIFICATIONS 41

APPENDIX B—UNCERTAINTY PROPAGATION THROUGH CALIBRATION REGRESSIONS 45

APPENDIX C—CALIBRATION RESULTS FOR THE ABSOLUTE PRESSURE TRANSDUCERS 51

FIGURES

1. Designs of LOFT absolute pressure transducers 6

2. Typical pressure transmission tube (standoff) for a LOFT absolute pressure transducer 8

3. Experimental pressure measurements within the reactor vessel 9

4. Experimental pressure measurements on the primary coolant loop 10

5. Experimental pressure measurements on the blowdown loop in the hot-leg-break configuration 11

6. Experimental pressure measurements on the blowdown loop in the cold-leg-break configuration 12

7. Experimental pressure measurements on the blowdown suppression system 13

8. LOFT absolute pressure measurement electronics 14

9. Power spectral density for PE-PC-4 during the Test L1-3A subcooled blowdown 33

TABLES

1. Zero-offset extremes summary 22

2. Measured and calculated resonant frequencies for the transducer standoff tubes on the primary coolant system 32

3. Absolute pressure measurement system response times 35

4. Summary of absolute pressure measurement uncertainties 37

C-1. Calibration results for the wide-range transducers 54

C-2. Calibration results for the narrow-range transducers 55

C-3. Calibration results for the 0.69-MPa transducers 56

C-4. Calibration results for the 3.48-MPa transducers 57

LOFT EXPERIMENTAL MEASUREMENTS UNCERTAINTY ANALYSES VOLUME X ABSOLUTE PRESSURE MEASUREMENT UNCERTAINTY ANALYSIS

1. INTRODUCTION

EG&G Idaho, Inc., is conducting the Loss-of-Fluid Test (LOFT) Program for the U.S. Nuclear Regulatory Commission as part of a broad study of nuclear reactor safety. The LOFT Program and the LOFT test reactor are specifically designed to obtain data applicable to loss-of-coolant accidents in commercial pressurized water reactors. To this end, numerous instruments are used to monitor nuclear, thermal, hydraulic, and structural behavior of the LOFT reactor during each loss-of-coolant experiment (LOCE).

Data from these instruments are of limited value without an assessment of how "accurate" or "reliable" these data are. All internal and external reports of LOFT test results show all measured and calculated quantities with their respective uncertainty intervals. These intervals are generally calculated at a minimum level of 95% confidence; that is, the confidence intervals surrounding the reported values will contain the true values in at least 95% of all cases.

Detailed performance appraisals of each type of monitoring device are required in order to facilitate timely calculation of confidence intervals for reported quantities. With this objective in mind, the LOFT Measurements Division has published a series of documents that evaluate sources of uncertainty for all categories of LOFT instruments. These reports are updated when significant changes in measurement hardware, procedural methods, or techniques of uncertainty estimation occur. The purpose of this report is to revise the analysis of uncertainties pertaining to absolute pressure transducers; thus, this document supersedes Supplement 9, Rev. A, to LOFT Technical Report 141-39.

The LOFT experimental absolute pressure transducers each utilize a diaphragm, backed by a sealed reference chamber, to sense pressure variations transmitted from the measurement location to the transducer by water-filled standoff tubes. Attached to the diaphragms are strain gages, which convert diaphragm deflections into electrical signals. These voltages are conditioned, amplified, recorded, and finally converted by computer into pressure readouts. Detailed descriptions of the transducer hardware and electronics, as well as specific transducer locations within the LOFT system, are supplied in Section 2 of this report. The specification requirements used to procure the transducers are presented in Appendix A.

1.1 Absolute Pressure Measurement Applications

Absolute pressure data are second in importance only to temperature data in the interpretation of thermal-hydraulic behavior during a LOCE. The transducers are used in general to measure shock loads from decompression and to assist in determination of coolant flow and fluid conditions. The transducers are also used to establish steady-state conditions before transient initiation and to evaluate responses from other instruments during pre-LOCE testing. The end-use of the transient data is to verify or improve existing computer models that predict various aspects of reactor response to a loss-of-coolant accident (LOCA).

1.1.1 Reactor-Vessel Measurements. The reactor core is more susceptible to damage from a LOCA than any other major component in a nuclear reactor. Sudden pressure loads from an abrupt decompression have the potential of warping fuel modules and distorting control rod channels, as well as fracturing core barrel welds. These loads must be thoroughly characterized for design safety assessments, and obtaining the required measurements is the primary goal of the absolute pressure sensors for the reactor vessel.

Removal of decay heat from the core after the reactor has scrammed is also a major consideration. Depressurization and diversion of a portion of the primary coolant disrupt normal coolant flow paths and alter the rate of convective heat removal. At any time, the magnitude of the core coolant flow is determined by the differential pressure measurements across the core and by the coolant momentum. Though several differential pressure sensors are installed on the reactor vessel, the long transmission lines required for these instruments make them inherently slower in response than the absolute pressure transducers. Since subcooled decompression and the associated pressure loads are particularly rapid phenomena, differences between absolute pressure transducer outputs provide more accurate differential pressure information during the subcooled phase of a transient. The absolute pressure transducers also provide useful backup data during the relatively slower saturated blowdown.

Several types of LOCA's cause the coolant level within a reactor vessel to drop significantly. Once the saturated blowdown is complete, a reflood phase is initiated in these types of transients to restore the coolant level. Details of the reflood timing and of localized variations in reflood effects are of interest for certain computer code studies. Several narrow-range, high-resolution absolute pressure transducers are located on the reactor vessel to make pertinent measurements. These instruments are particularly sensitive to the additional pressure caused by the weight of the coolant entering the vessel during this phase of certain LOFT tests.

1.1.2 Primary-Coolant-Piping-System Measurements. The absolute pressure transducers installed on the primary system piping (the portion of the primary coolant system that excludes the reactor vessel) are used more for studying coolant behavior than for evaluating hazards from sudden pressure loads. As in the core, the coolant flow alters in response to changing differential pressures, and absolute pressure instruments are critical to the understanding of flow changes immediately following transient initiation. Heat-transfer properties are perturbed by the steam formation accompanying depressurization, and absolute pressure data are essential to the analysis of the associated fluid transformation into a complex two-phase mixture. In addition, absolute pressure measurements are made at the inlets and outlets of the reactor vessel and near the primary coolant pumps to aid in interpretation of velocity, density, and temperature measurements at these locations.

Two of the transducers on the primary piping are relatively immune to drift due to a special technique for attaching strain gages to their diaphragms. These transducers are used as references for the other primary-coolant-system absolute pressure transducers during pre-LOCE pressure testing. Output voltages are obtained from all primary system transducers, with the exceptions of the narrow-range instruments, at six LOFT system pressures spanning the range of interest. The reference transducer voltages are converted by software into engineering units. These pressures are averaged, and sets of voltages from individual transducers are fitted against the reference (average) pressures by least-squares regression. This calibration process detects any transducer drift that has occurred since the last LOFT test. The offset and slope coefficients for any transducers exhibiting drift are modified accordingly. The narrow-range reactor-vessel transducers described earlier can be checked at only one of the six test points; consequently, the comparison of their output voltages against the lowest reference pressure serves only as an offset coefficient calibration.

The uncertainty analysis for the two reference transducers is presented in Section 3 of this report. Sections 4 and 5, respectively, provide the analyses for the wide- and narrow-range transducers used with the primary-coolant-system. Section 4 relies heavily on a study of uncertainty propagation through the least-squares regression process, and this study is presented in Appendix B. Laboratory calibration data, which are used extensively in Sections 4 and 5, are tabulated in Appendix C.

1.1.3 Blowdown-Suppression-System Measurements. In an actual LOCA, water escaping the primary coolant system would reach the containment building floor. To prevent possible contamination of the LOFT containment, primary coolant, during a LOCE, is discharged into a blowdown suppression system which consists of a large storage tank and a header connecting the blowdown valves to the tank. The suppression system is instrumented for measurement of coolant level in the tank and measurement of break flow rate during a simulated LOCA.

Two different ranges of absolute pressure transducers have been installed on the blowdown suppression system. Two 0- to 3.48-MPa transducers are mounted near the blowdown valves, while 0- to 0.69-MPa devices measure tank and header pressures. Both ranges of transducers measure pressure loads from decompression on the structures to which they are attached. The suppression system is closed to the atmosphere and presents an increasing backpressure to the break flow over the transient duration; both ranges of transducers are used to characterize this boundary condition for certain transient phases such as reflood. The header transducers also assist in determining the system pressure decay at the break location.

The uncertainty analyses for both ranges of blowdown-suppression-system measurements are presented in Section 6 of this report. Manufacturer's calibration data are used extensively in the analyses, and these data are contained in Appendix C.

1.2 Absolute Pressure Measurement Requirements

Two overlapping documents list requirements on performance levels for the LOFT absolute pressure measurements. These documents are the System Design Description of the Test Assembly Experimental Measurements System,[1] and the Measurement Requirements Document.[2] Reference 1 reflects performance levels desired from the plant analysis standpoint, while Reference 2 is oriented toward accuracies needed for computer model verifications. Neither document considers limitations imposed by the reactor environment and by state-of-the-art instrument performance. Consequently, the "requirements" to be described are to be interpreted as goals to be met, if at all possible, rather than as legalistic mandates.

The measurement requirements may be separated into areas of accuracy and response. Accuracy requirements limit the magnitude of uncertainty (confidence) intervals, and response requirements restrict acceptable lag times. Measurement response behavior is evaluated in detail in Section 7 of this report. Section 8, which summarizes uncertainties and response characteristics for the LOFT absolute pressure measurements, assesses compliance of the transducers to the requirements that follow.

1.2.1 Accuracy. The accuracy limits include considerations of uncertainties from calibration, signal conditioning, data recording, and procedural data-handling methods. All values are given at the 95% confidence level.

Reference 1 lists a requirement of 1.0 RG (percent of range) for the reactor-vessel and other primary-coolant-system measurements. The ranges of these measurements are 0 to 17.24, 0 to 20.69, and 0 to 1.38 MPa for the reference, wide-range, and narrow-range transducers, respectively. The corresponding accuracy requirements are ±172.4, ±206.9, and ±13.8 kPa. Reference 1 has no requirement for pressure measurements on the blowdown suppression system. Reference 2 limits measurement uncertainties to within ±(90 kPa + 5RD) for the primary coolant system and to within ±(1.8 kPa + 5RD) for the blowdown suppression system, where RD stands for percent of reading.

1.2.2 Response. Limits on acceptable reponse times are necessary to ensure that the LOFT absolute pressure transducers are able to measure rapid aspects of LOFT transients. The limits that follow cover the amplifying, interfacing, and data recording equipment, as well as the transducer hardware. The response time criteria are specified in terms of maximum allowable (upper limit) rise times. Rise time is defined as the time necessary for a measurement system to go from 10 to 90% of a full-scale step function.

Reference 1 requires measurement system rise times less than 500 milliseconds for the primary coolant system and, again, makes no requirement for the blowdown suppression system. Reference 2 limits rise times for the primary coolant system to 30 ms for subcooled blowdown and to 850 ms for saturated blowdown. The Measurement Requirements Document also limits rise times for the blowdown suppression system to 150 ms during all phases of a LOCE transient.

2. DESCRIPTION

The LOFT Program has purchased five distinct transducer groups from a total of three manufacturers to obtain absolute pressure measurements on the LOFT reactor during transient tests. These groups are the wide- and narrow-range Teledyne Taber transducers, the 0.69- and 3.48-MPa Precise Sensors transducers, and the Bell and Howell reference transducers. The Teledyne Taber, and Bell and Howell transducers are mounted on the LOFT primary coolant system, while the Precise Sensors transducers are installed on the blowdown suppression system. Output voltages from these transducers are amplified and recorded for later analysis on two different data-handling systems, the Digital Data Acquisition and Processing System (DDAPS) and the Wide Band Frequency Modulated System (WBFM). A third system, the Digital Data Acquisition System (DDAS) is also used for measurement redundancy; however, an appropriate uncertainty analysis has not yet been performed for this system, and this document neither includes nor describes DDAS uncertainties. (Until a detailed analysis of the DDAS has been performed, DDAPS uncertainty values will be used for measurements recorded on the DDAS.)

The subsequent material within this section describes the mechanical operation, specific installation locations, and the electronic principles of the absolute pressure transducers. Pertinent details of the data-handling electronics are also provided.

2.1 Transducer Hardware

Each of the LOFT absolute pressure transducers utilizes four strain gages, a diaphragm, and an evacuated reference chamber to monitor pressure. Pressure on the system side of the transducer forces the diaphragm to deflect, since the reference chamber is on the other side of the diaphragm. The deflection is transmitted either directly or indirectly to the strain gages, which respond by changing resistance. The four gages are connected electrically in a Wheatstone Bridge configuration; the bridge is nominally balanced with zero pressure on both sides of the diaphragm. Thus, any significant pressure on the system side unbalances the bridge and induces a potential difference across the bridge. This potential difference is the transducer output voltage.

Different approaches to mounting strain gages and transmitting diaphragm deflections are used, depending on the particular manufacturer and the transducer pressure range. The three general approaches are displayed in Figure 1.

The most straightforward arrangement is shown in View 1-A for the 20.69-MPa (wide-range) Teledyne Taber and 17.24-MPa Bell and Howell transducers. The strain gages are mounted directly on the reference side of the diaphragm. When the diaphragm deflects, radial strains near the diaphragm periphery are under compression relative to the tension strains near the diaphragm center. Compression strains decrease gage resistance and tension strains increase resistance. The only significant difference in construction between the two manufacturers is the method of strain gage attachment. Teledyne mounts the gages to the diaphragm by a combination of heat and pressure; Bell and Howell deposits the gage material by sputtering over a detachable mask. The sputter-deposited bond is less prone to formation of small delaminations during use, resulting in enhanced stability.

View 1-B shows the method of construction for the 1.38-MPa (narrow-range) Teledyne Taber transducers. These instruments are subject to lower pressures and smaller diaphragm displacements than the wide-range transducers; however, the strain gages are nominally the same. In order to keep the full-scale output voltages equivalent at 30 millivolts, mechanical amplifying arms are required. As shown, the strain gages are positioned for a tension/compression bridge imbalance comparable to that for the wide-range transducers.

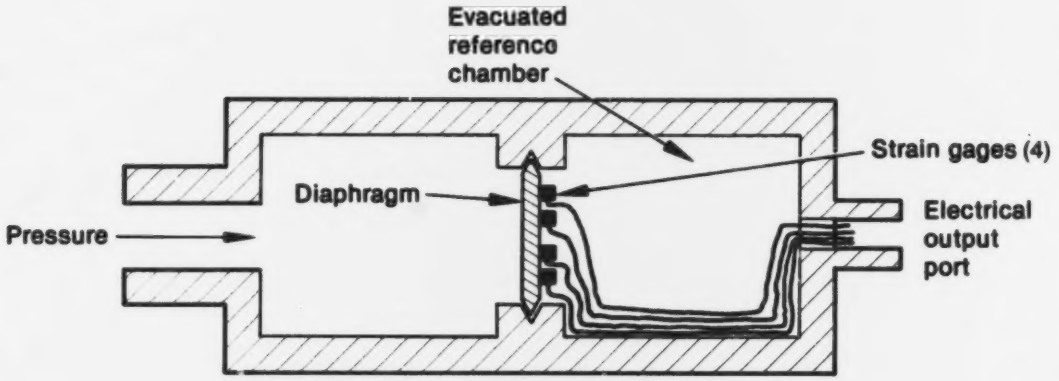

1-A. 20.69-MPa Teledyne; 17.24-MPa Bell and Howell.

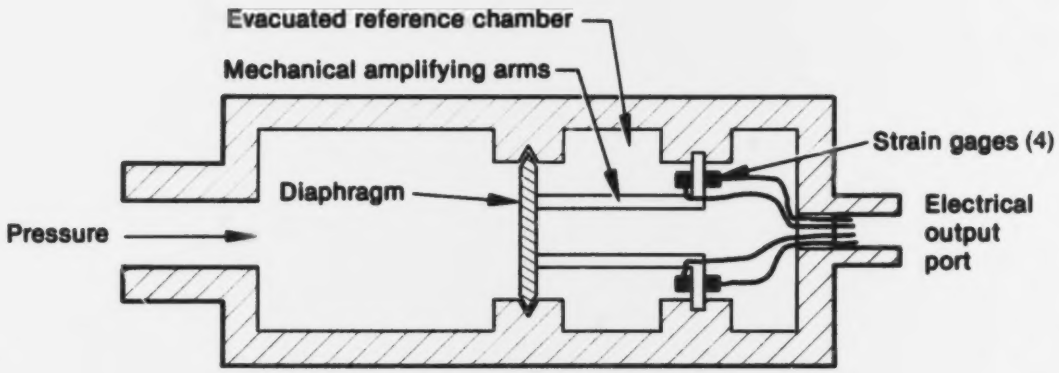

1-B. 1.38-MPa Teledyne.

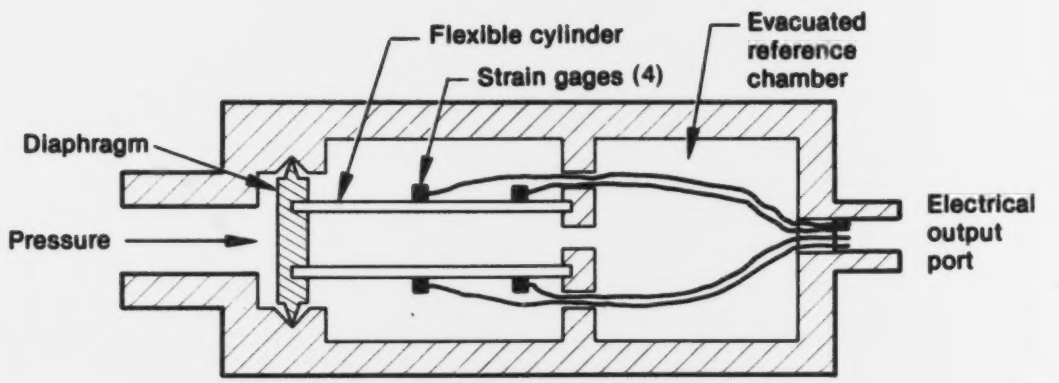

1-C. 3.48 and 0.69-MPa Precise sensors.

INEL-A-18 249

Figure 1. Designs of LOFT absolute pressure transducers.

View 1-C illustrates the design of the Precise Sensors Inc. transducers that measure pressure within the blowdown suppression system. In response to system pressure, the diaphragm forces the flexible cylinder to assume a convex shape. Strain gages mounted near the cylinder center are in tension with respect to those mounted near the end, and a bridge imbalance results. The strain gages are attached to the flexible cylinder by combination of heat and pressure.

In terms of performance characteristics, there are many differences between the five transducer groups beyond the design distinctions. These differences, as well as performance similarities, are summarized in Appendix A. This appendix contains the performance specifications used to procure the transducers. As noted in the appendix introduction, the specifications follow manufacturer's product literature and, thus, reflect actual device characteristics closely.

2.2 Transducer Installation

With the exceptions of the blowdown-suppression-system transducers, which are screwed directly into threaded holes in the suppression tank and header, all other LOFT absolute pressure transducers are mounted on 6.35-mm diameter standoff tubes in a typical configuration as shown in Figure 2. Accurate pressure measurements require that each standoff be filled with water and be free of trapped air bubbles. The series of manual valves shown on Figure 2 are used to bleed air from the standoff in preparation for each LOFT test. The valves are also used periodically to isolate the transducer in order that an in-place calibration check be performed by attaching an external pressure source.

More Precise Sensor and Teledyne Taber transducers have been purchased than are actually installed on the LOFT reactor at any given time. Occasionally, pressure transducers must be removed for repair or recalibration; consequently, a supply of spare transducers is necessary. Only 14 of the 32 wide-range Teledyne, three of the 10 narrow-range Teledyne, two of the four 3.48-MPa Precise Sensor, and 11 of the 16, 0.69-MPa Precise Sensor transducers available are actually in use at this writing. Because spare transducers are placed into service, uncertainties calculated later in this report will reflect laboratory calibration data from the entire population of purchased transducers, rather than from only those currently installed.

2.2.1 Primary Coolant System. The primary coolant system may be divided into three subsystems: the reactor vessel, the primary coolant loop, and the blowdown loop. The reactor vessel houses the core; the primary coolant (operating) loop serves to control coolant flow, pressure, and temperature within the LOFT reactor; and the blowdown loop simulates hot- or cold-leg breaks in a typical pressurized water reactor.

Figure 3 displays a side view of the five wide-range and three narrow-range absolute pressure transducer locations within the reactor vessel. As shown, the locations are such that pressure differences across the core and between several elevations can be determined. The "station" markings on the left side of the figure are a relative measure of elevation differences in units of inches.

Figure 4 presents a top view of the primary coolant loop. Wide-range transducers PE-PC-1, PE-PC-2, and PE-PC-4 measure cold-leg (reactor-vessel-inlet) pressure, hot-leg (reactor-vessel-outlet) pressure, and pressurizer pressure, respectively. Transducers PE-PC-5 and PE-PC-6 monitor steam-generator-outlet pressure, as well as serving as references for the other primary-coolant-system instruments during pre-LOCE pressure testing.

Figures 5 and 6 provide top views of the blowdown loop in the hot-leg-break and cold-leg-break configurations. (For convenience, both figures show the steam generator and pump simulators oriented horizontally; in fact, the steam generator simulator is vertically oriented in an inverted "U" position above the pump simulator.) In each configuration a total of six wide-range absolute pressure transducers determine pressure differences induced by the varying pipe areas and geometries as coolant escapes to the header during a break-type transient.

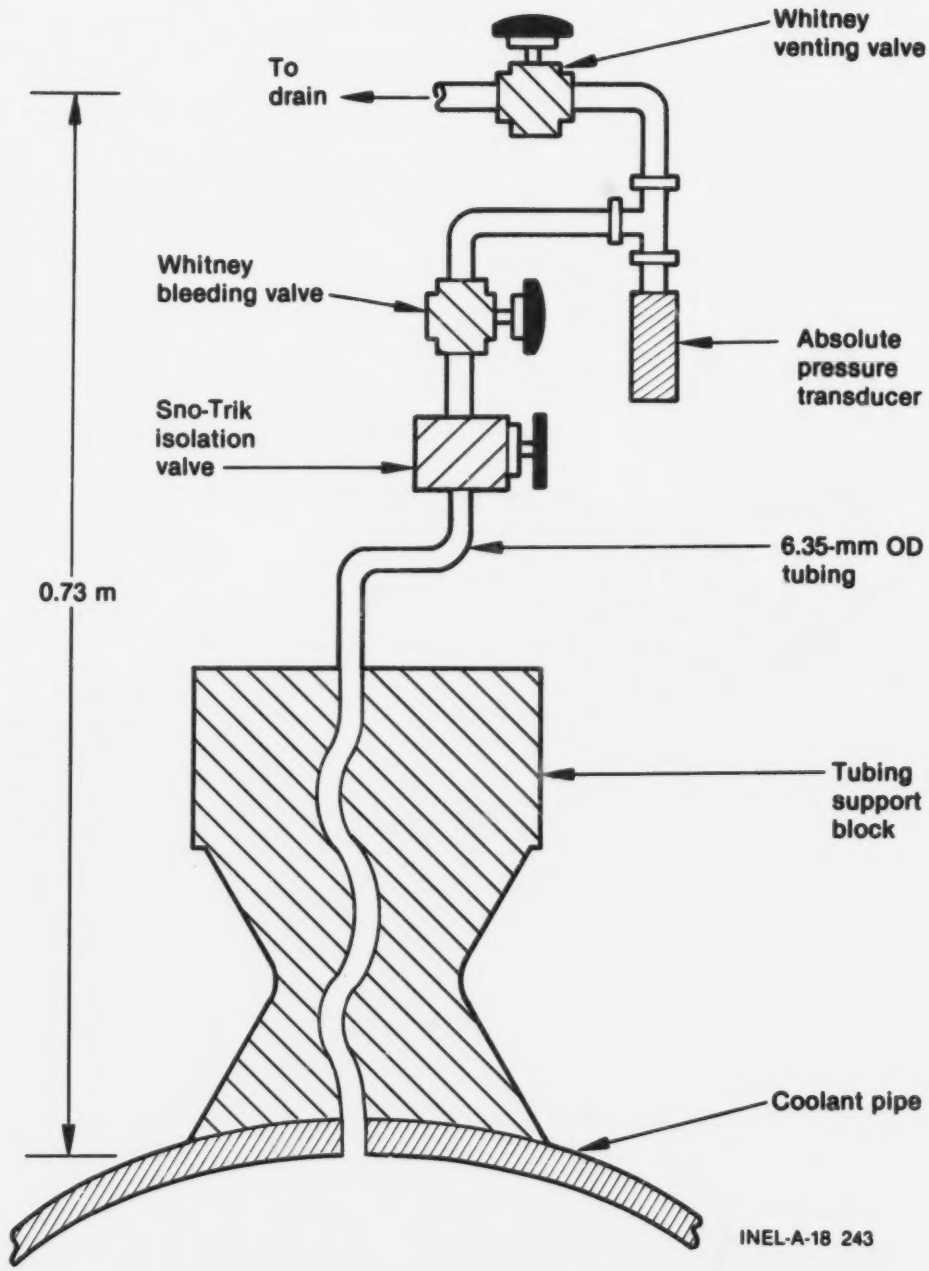

Figure 2. Typical pressure transmission tube (standoff) for a LOFT absolute pressure transducer.

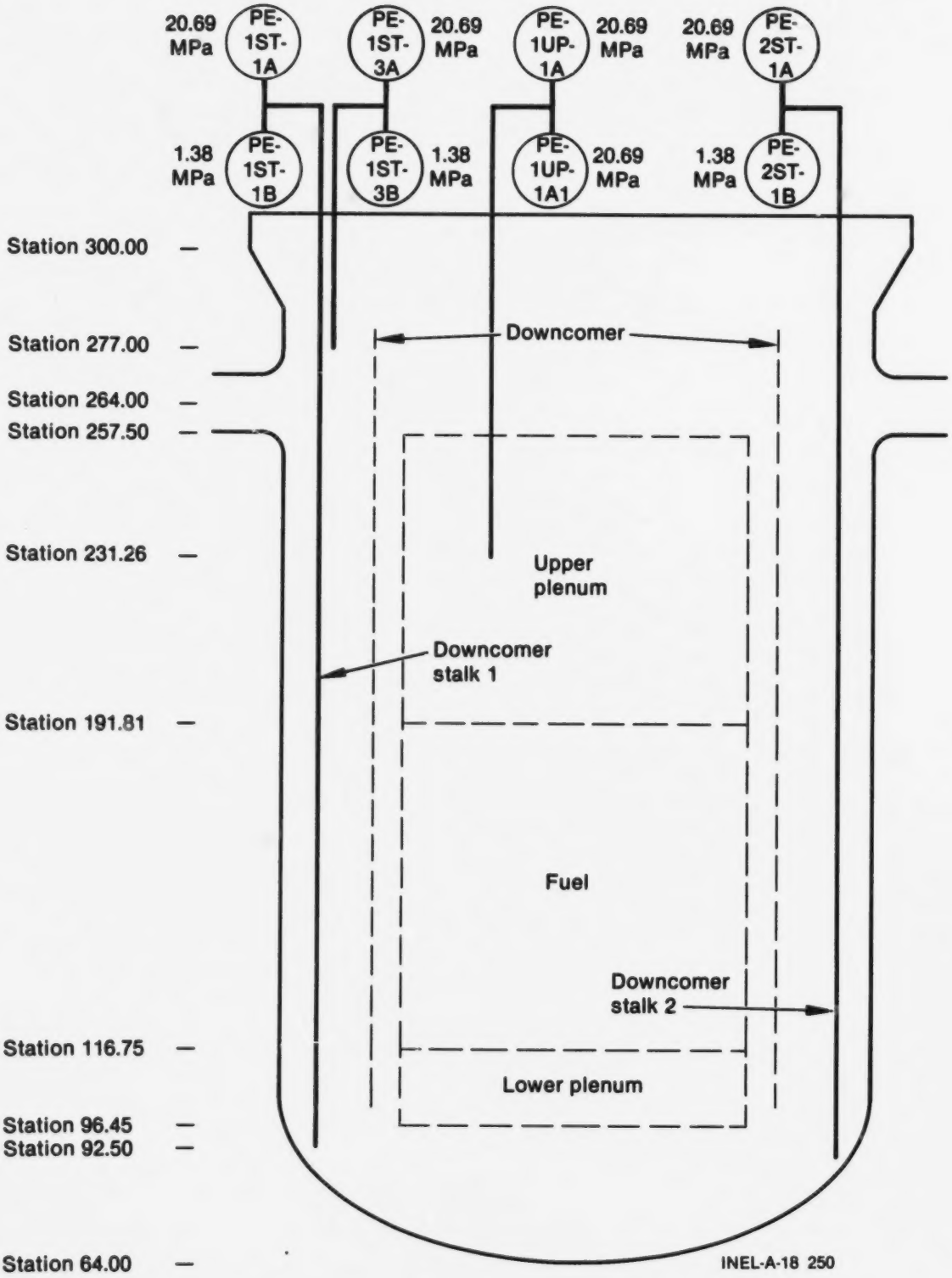

Figure 3. Experimental pressure measurements within the reactor vessel.

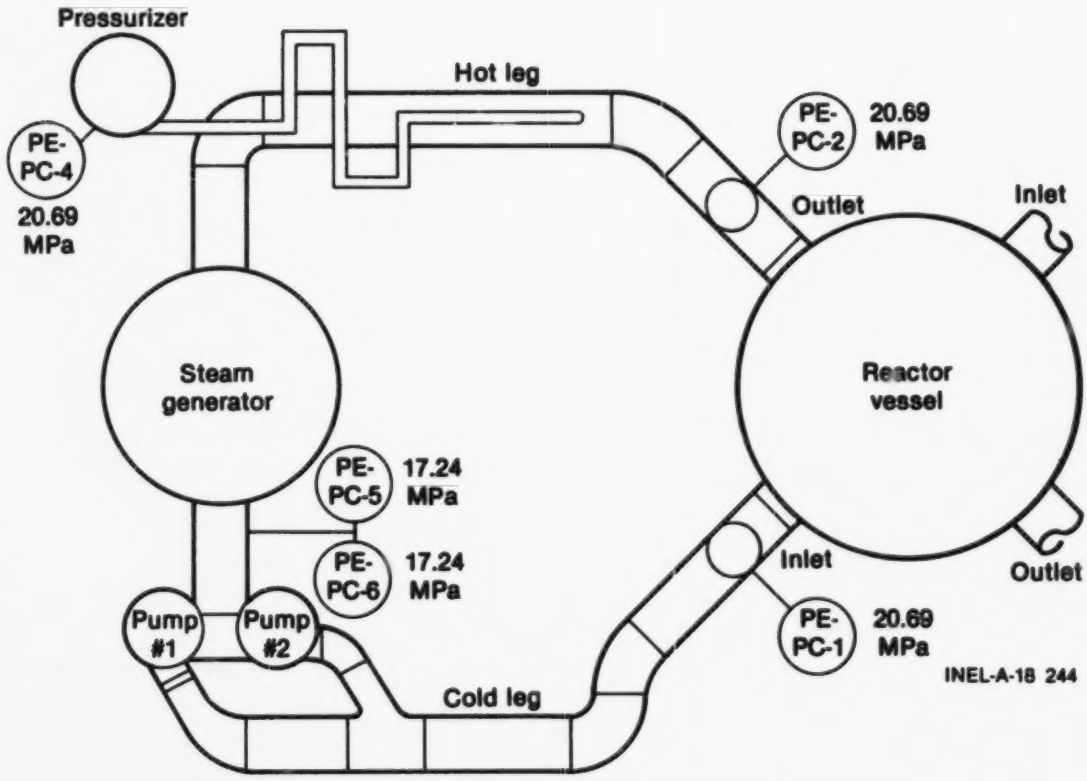

Figure 4. Experimental pressure measurements on the primary coolant loop.

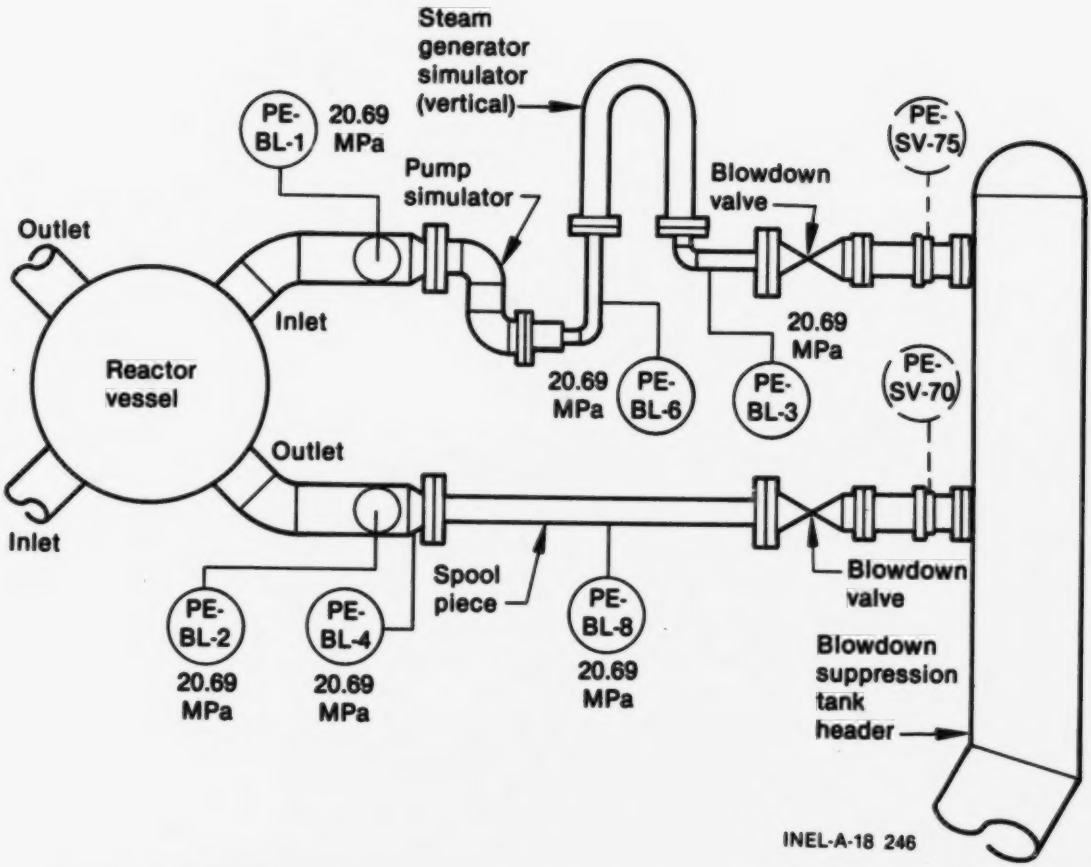

Figure 5. Experimental pressure measurements on the blowdown loop in the hot-leg-break configuration.

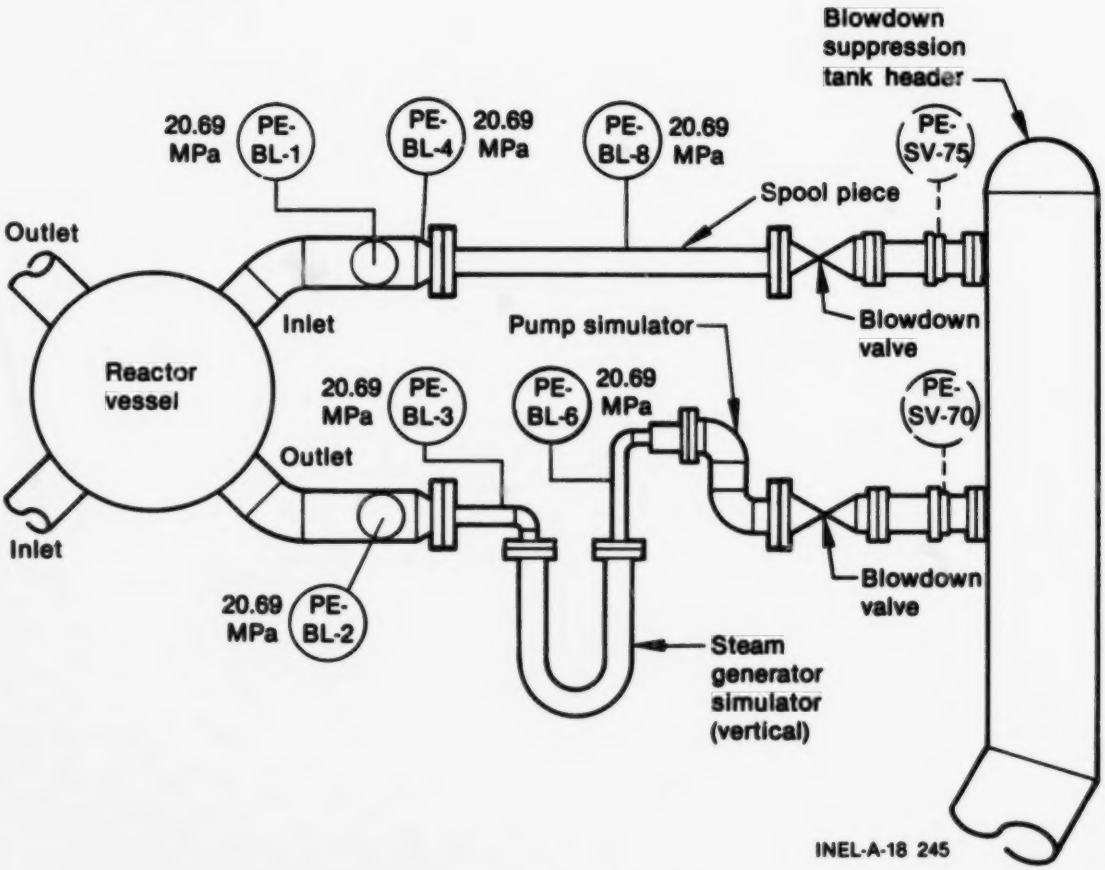

Figure 6. Experimental pressure measurements on the blowdown loop in the cold-leg-break configuration.

2.2.2 Blowdown Suppression System. Figure 7 illustrates the positions of the two 3.48-MPa and 11 0.69-MPa absolute pressure transducers installed on the blowdown suppression system. As shown, the 3.48-MPa transducers are installed on the relatively constricted blowdown valve connections. Contrariwise, the header and tank volumes, which are not subject to the large pressures near the blowdown valves, may be monitored by the more sensitive 0.69-MPa transducers.

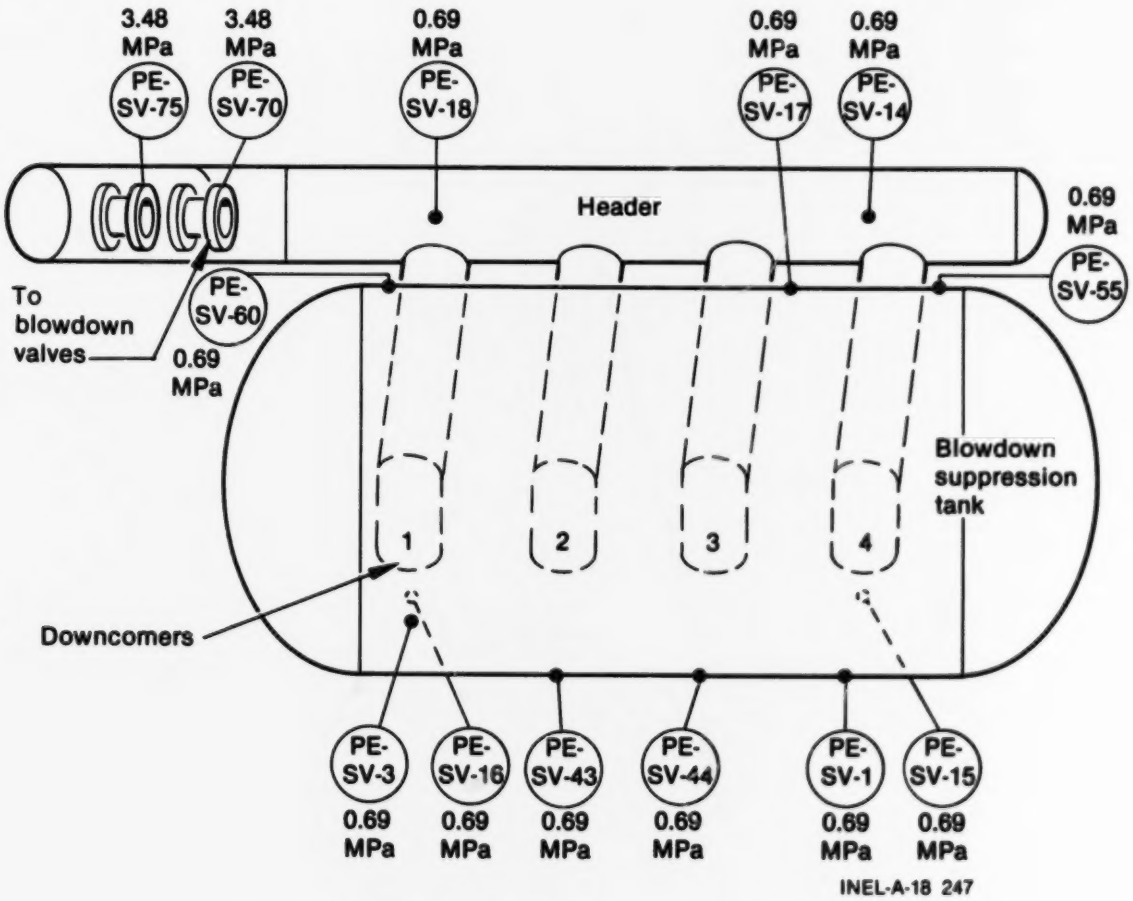

Figure 7. Experimental pressure measurements on the blowdown suppression system.

2.3 Measurement System Electronics

Data from the LOFT absolute pressure transducers are recorded on two types of systems. When fast recording response is necessary to follow particularly rapid pressure changes, the analog output voltages are fed into the Wide Band Frequency Modulated System (WBFM). When accuracy of voltage magnitudes is important and when the relatively slow response time of an analog-to-digital converter can be tolerated, the data are recorded on the DDAPS (or DDAS). Absolute pressure information from critical locations are frequently recorded on both types to ensure against any recording malfunctions.

Both recording systems are displayed on Figure 8. As shown, the voltage signals originating at each pressure transducer are sent to one or both systems by pretest manual selection at the low-level patch panel. Each system uses a differential amplifier to preamplify the signals and to eliminate common-mode noise.

After preamplifying, the WBFM simply records the data on analog tape. Alternatively, the DDAPS (and DDAS) convert the preamplified signals into digital form and route the signals through a computer to either a magnetic disk or tape, depending on the amount of data to be stored.

The recorded output voltages must be converted into engineering units for plotting and for meaningful data analysis. This conversion is performed by computer after test termination. Each pressure is yielded by an equation of the form $P = D_1 E + D_0$, where D_1 is the slope coefficient, E is the transducer output voltage, and D_0 is the offset coefficient. These slope and offset coefficients are determined for individual transducers by calibration against known standards. Details of calibration methods are given in subsequent sections of this report, where uncertainties pertaining to the calibrations are discussed.

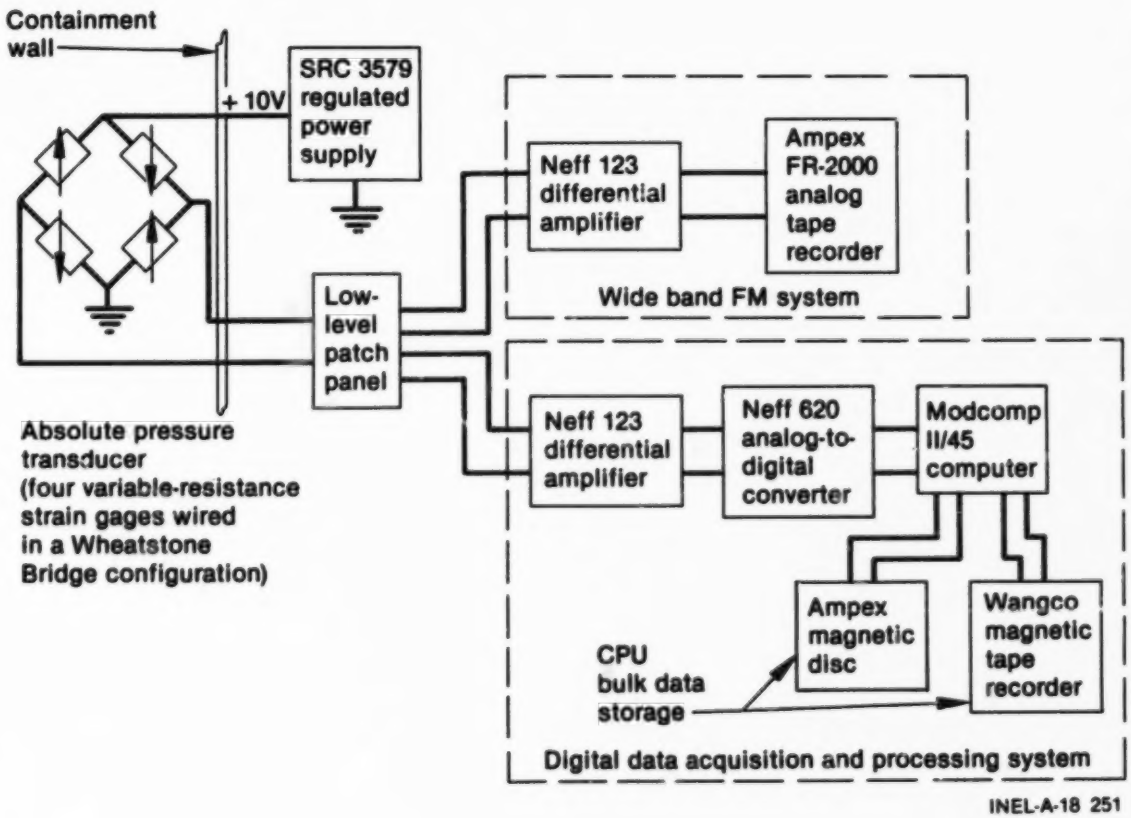
Containment wall
+ 10V
SRC 3579 regulated power supply
Neff 123 differential amplifier
Ampex FR-2000 analog tape recorder
Wide band FM system
Low-level patch panel
Absolute pressure transducer (four variable-resistance strain gages wired in a Wheatstone Bridge configuration)
Neff 123 differential amplifier
Neff 620 analog-to-digital converter
Modcomp II/45 computer
Ampex magnetic disc
Wangco magnetic tape recorder
CPU bulk data storage
Digital data acquisition and processing system
INEL-A-18 251

Figure 8. LOFT absolute pressure measurement electronics.

3. REFERENCE MEASUREMENTS

Two 0- to 17.24-MPa absolute pressure transducers, PE-PC-5 and PE-PC-6, are used as references for other pressure transducers in the primary coolant system. The strain gages in the reference transducers were attached to their diaphragms by sputter-deposition; this feature makes them more resistant to drift than the other mechanically-bonded strain gage transducers.

This increased stability by no means makes the reference transducers immune to error. Reference pressures, calculated in software from measured transducer output voltages, possess uncertainties associated with the calibration coefficients, with thermal variations in the transducer environment, with adjustments to local atmospheric pressure, and with output-voltage recording errors.

The uncertainty analysis for the reference measurements will proceed on a somewhat different basis than for the other transducer classes to be discussed in this report. The "reference" pressures are averages of the pressures calculated from the PE-PC-5 and PE-PC-6 output voltages. Reference pressure uncertainties are required for uncertainty calculations for the other transducers in the primary coolant system; estimating the uncertainty for the average requires separate computation of uncertainties for each reference transducer. The other classes contain up to 32 transducers, and limitations on time and space prohibit uncertainty analyses for individual transducers. Instead, worst-case approaches will be adopted.

3.1 Calibration and Traceability Uncertainties

The reference transducers were calibrated against a laboratory-standard pressure system at the Idaho National Engineering Laboratory (INEL). The results, after the coefficient standard errors were multiplied by the appropriate two-tailed Student's T Table value ($t_{61,0.025} = 2.00$; 63 calibration data points) for conversion into 95% confidence intervals, are as follows:

		Zero Offset (D_0)	Slope Coefficient (D_1)
PE-PC-5			
	300 K	-0.036 ± 0.016 MPa	564.7 ± 0.9 MPa/V
	343 K	-0.062 ± 0.016 MPa	566.0 ± 0.9 MPa/V
PE-PC-6			
	300 K	0.080 ± 0.015 MPa	585.0 ± 0.9 MPa/V
	343 K	0.035 ± 0.015 MPa	584.0 ± 0.9 MPa/V

The Gilmore Model 289 system used for calibration is traceable to the National Bureau of Standards with an uncertainty (95% confidence) of 0.114% of reading. Inclusion of this uncertainty by root-sum-squaring has a negligible effect on the D_0 uncertainties, but does change the slope coefficient uncertainty to ±1.1 MPa/V at both temperatures for both transducers.

In order to obtain a total uncertainty for either transducer from the uncertainty values listed above, it would first be necessary to multiply the slope coefficient uncertainty by the output voltage at the pressure desired. However, the transducer output voltages are not conveniently available, having been converted in software to pressures for plotting or tabulation. Instead, the MPa/V-uncertainties may be divided by the

respective D_1 values and then multiplied by 100; the MPa/V-uncertainties are thereby converted into percentages of reading (RD) uncertainties. To calculate a total uncertainty at a given pressure, the RD uncertainty is conveniently multiplied by the pressure (directly available from a plot) and the product is added to the offset uncertainty (already in a convenient form).

The slope uncertainty (1.1 MPa/V) converts to 0.195 RD for PE-PC-5 and to 0.188 RD for PE-PC-6. Because a convention exists whereby uncertainties are reported with only two significant digits, the uncertainties associated with the reference transducer slope coefficients are conservatively approximated as ±0.20 RD for PE-PC-5 and as ±0.19 RD for PE-PC-6 for inclusion in the summary table (Table 4).

3.2 Thermal Variations

The laboratory calibration results reported in the previous section show that the reference transducer characteristics are temperature-dependent. This dependence is a source of uncertainty in that the ambient temperature in the immediate vicinity of the LOFT reactor is not stable. As the reactor coolant is heated in preparation for a transient test, the temperature of the surrounding air and of the transducer mountings rises, also. Thermocouples were mounted on transducer bodies prior to Test L1-4 in order to assess the amount of the ambient temperature increase. The largest increase found among the transducers checked was approximately 20 K over the duration of the pretest and test activities.

Interpolation of the coefficient values listed in Section 3.1 suggests that a 20-K increase would cause transducer performance shifts measured by the following coefficient biases:

	D_0	D_1
PE-PC-5	-0.012 MPa	0.6 MPa/V = 0.105 RD
PE-PC-6	-0.021 MPa	-0.5 MPa/V = 0.086 RD

Because only the 300-K calibration coefficients are used to convert output voltages to pressures, the above biases must be regarded as uncertainties in the coefficients.

3.3 Absolute Pressure Adjustment

The reference transducers are prone to offset drifts. The following procedure has been adopted to counteract any such drifts and to ensure that the reference pressures are truly in terms of absolute pressure. Prior to each pre-LOCE pressure test, the reference transducers are valved-off and vented to the atmosphere. The transducer amplifiers are then zeroed such that atmospheric pressure at that time yields a null output at the amplifier stage. Adjustments equal to ambient containment pressure are made in software during the pressure tests and after the LOFT tests themselves. This process lowers the measured output voltages instead of altering the D_0 values, and the adjustment values should be regarded as additional factors in the software calculations of the reference transducer pressures. For purposes of this document, the adjustment values will be treated as D_0 modifications since the net effect with respect to offset uncertainty is the same.

Ambient containment pressure is determined by averaging the responses of three process pressure transducers, PT-P120-41, -42, and -43. Each response used in the average is procedurally required to be between 0.083 and 0.090 MPa, a range that brackets local atmospheric pressure variations, or the response is discarded. Since no other procedural controls or calibration methods have been implemented for these three process transducers, a worst-case offset uncertainty of ±0.007 MPa must be assumed.

Because realistic offset values are necessary for later calculations, a positive adjustment value of 0.086 MPa is assumed for both reference transducers. Incorporating this value with the D_0 values from Section 3.1 yields nominal D_0 values of 0.050 MPa for PE-PC-5 and 0.166 MPa for PE-PC-6.

3.4 Data Recording Errors

Absolute pressure transducer output voltages are recorded on two types of systems for later conversion by software into engineering units. Which system is used depends on the response time necessary and the end-use of the data. The 95% confidence levels are reported in Reference 3 as 0.13 RG (percent of measurement range) for the DDAPS and as 1.1 RG for the WBFM. Since the measurement range is identical to the transducer range for all of the absolute pressure transducers and since the range of the reference transducers is 0 to 17.24 MPa, the data recording uncertainties are ±0.022 and ±0.190 MPa, respectively. Because these values are independent of the pressure being measured, they must be treated as zero-offset uncertainties.

3.5 Reference Measurement Summary

The overall uncertainties in the pressures calculated from the reference transducer output voltages are obtained by combining the results of the preceding sections. The transducer temperature variations induce biases in the transducer performance characteristics, and the uncertainties in both the offset and slope coefficients from this source are combined with the calibration uncertainties by arithmetic addition. This yields D_1 uncertainties of $^{+0.300}_{-0.195}$ RD for PE-PC-5 and $^{+0.188}_{-0.274}$ RD for PE-PC-6 and D_0 uncertainties of $^{+0.016}_{-0.028}$ MPa for PE-PC-5 and $^{+0.015}_{-0.036}$ MPa for PE-PC-6. Zero-offset uncertainties from the absolute pressure adjustments and from the data recording systems are largely attributable to random errors; therefore, these values must be separately combined with the asymmetrical offset limits listed above by root-sum-squaring. After conservatively rounding-off the uncertainty values to two significant digits, the nominal reference transducer coefficients and uncertainties are as follows:

	D_0 (DDAPS)	D_0 (WBFM)	D_1
PE-PC-5	0.050 $^{+0.028}_{-0.036}$ MPa	0.050 ± 0.200 MPa	564.7 MPa/V $^{+0.30}_{-0.20}$ RD
PE-PC-6	0.166 $^{+0.028}_{-0.043}$ MPa	0.166 ± 0.200 MPa	585.0 MPa/V $^{+0.19}_{-0.28}$ RD

The primary-coolant-system reference transducers form a distinct class, by virtue of both their uncertainty magnitudes and their measurement range, from other absolute pressure transducers analyzed in this report. Consequently, uncertainty results for these two transducers must be combined for inclusion in the final summary table (Table 4), as is the case for the other classes of transducers. For summary table purposes, it is most convenient to express uncertainties in terms of a single symmetric limit wherever possible. Conservative values which bracket the individual transducer uncertainties are ±0.043 MPa on the zero offset (DDAPS recording), ±0.20 MPa on the zero offset (WBFM recording), and ±0.30 RD on the measured pressure.

4. WIDE-RANGE MEASUREMENTS

The wide-range (0- to 20.69-MFa) transducers are the most significant class of absolute pressure transducers analyzed in this report. Sensors of this type are installed throughout the primary coolant system, and most of the absolute pressure information pertaining to thermal-hydraulic behavior of the LOFT reactor is obtained from them. It will also become apparent from the subsequent analyses of the remaining transducer classes that the reference transducers are intended for on-line calibration checks of the wide-range transducers only. This emphasis reflects the overwhelming importance of wide-range transducer experimental data.

Data from the wide-range measurements have uncertainties arising from three primary sources: (a) errors in the calibration coefficients used in software for calculations of pressure from measured output voltages, (b) output-voltage recording errors, and (c) height differences between certain of the wide-range transducers and the reference transducers. These sources will be described in detail in the following sections.

Transducer temperature variations, of the sort described in Section 3.2, are not a separate source of error for these devices. The wide-range transducers are calibrated at operating temperature against the reference transducers. Thus thermally-induced changes from a laboratory calibration are not a factor. Temperature variations in the reference transducers create error in the calibration coefficients, but this error is accounted for in the following section.

4.1 Calibration Coefficient Uncertainties

The wide-range absolute pressure transducers are calibrated against the reference transducers, PE-PC-5 and -6, during two separate phases of the pre-LOCE testing. The first phase, called the cold pressure test, occurs early in the pre-LOCE activities at coolant temperatures less than 366 K. The second calibration occurs during the hot pressure test, shortly before the LOFT reactor attains criticality, at a coolant temperature of approximately 555 K. Both the hot and cold pressure tests are performed with no coolant flow, and the reference transducers are vented and set to ambient pressure (see Section 3.3) before both tests.

The transducer calibration procedure is essentially the same during both testing phases. Output voltages from the wide-range and reference transducers are recorded on the DDAPS at the six system pressures. Pressures are calculated for PE-PC-5 and -6, using the calibration coefficients discussed in Section 3, and these values are averaged to provide the six reference pressures. The set of six output voltages from each wide-range transducer are fitted by linear least-squares regression against the six reference pressures. The slope (D_1) and the y-intercept (D_0) of the line generated by the fitting process are compared against the wide-range transducer coefficients used in the previous LOFT test. (The comparison is made against laboratory calibration values for newly installed transducers.) If a statistically significant difference is found to exist, transducer drift has occurred and the new coefficient value is entered into the LOFT Control Records. Additional information on the pre-LOCE calibration procedures is provided in Reference 4.

The linear least-squares regression process is described in detail in Appendix B. General calibration coefficient equations for the wide-range transducers are derived in terms of the six nominal reference pressures, nominal wide-range transducer output voltages at these nominal pressures, and deviations from both sets of nominal values. Appendix B assumes that any off-nominal deviations may be described as combinations of offset biases and pressure-dependent errors. Consequently, limits may be placed on the magnitudes of any such deviations by separately bounding offset and pressure-dependent uncertainties. Since both wide-range and reference transducers are involved in the wide-range transducer calibration, four factors are required to account for all of the types of variation encountered.

Section 3 coupled all pressure-dependent uncertainty magnitudes from the reference transducers to the respective slope coefficient values such that the magnitudes were converted into percentage of pressure uncertainties; these RD values will be used in the estimation of reference calibration uncertainties. A similar approach will be used for the pressure-dependent uncertainties from the wide-range transducers. However, since wide-range transducer output voltages are used as input to the calibration regressions, the RD uncertainties will be percentages of the measured voltage instead of percentages of pressure.

The Appendix B equations are:

$$D_o = CS\ (1.467 \times 10^{-3}\ \text{MPa}) + KS\ (1.000) - BC\ (689.54\ \text{MPa/V}) \quad (1)$$

and

$$D_1 = C/S\ (689.54\ \text{MPa/V}) \quad (2)$$

where

K = the constant offset in the reference pressures

$$C = 1 \pm \frac{\text{the RD uncertainty in the reference pressures}}{100}$$

B = the constant offset in the wide-range transducer output voltages

$$S = 1 \pm \frac{\text{the RD uncertainty in the output voltages}}{100}.$$

The meaning of these four factors will be further clarified in the following subsections, where confidence intervals will be estimated for each factor.

4.1.1 The K Factor. Separate zero-offset uncertainties for the reference transducers have already been calculated in Section 3. The 95% confidence values (DDAPS recording during all pre-LOCE tests) on the offsets are $0.050\ ^{+0.028}_{-0.036}$ MPa for PE-PC-5 and $0.166\ ^{+0.028}_{-0.043}$ MPa for PE-PC-6. Because reference pressures are averages of the pressures calculated from the two transducer output voltages, offset uncertainty values appropriate to the averages must be calculated. The correct propagation of errors formula is

$$\sigma_{AV}^2 = \left(\frac{1}{2}\right)^2 \sigma_5^2 + \left(\frac{1}{2}\right)^2 \sigma_6^2 \quad (3)$$

where σ is a 95% confidence value and not a standard deviation. The average zero-offset and 95% confidence bounds on the average are $0.108\ ^{+0.020}_{-0.028}$ MPa. Thus, the 95% confidence limits on K are 0.080 and 0.128 MPa.

4.1.2 The C Factor. Uncertainties having confidence intervals dependent on the value of the pressure being measured were combined for the reference transducers in Section 3. When expressed in terms of percents of reading, these uncertainties are $^{+0.30}_{-0.20}$ RD for PE-PC-5 and $^{+0.19}_{-0.28}$ RD for PE-PC-6. These values must be combined according to Equation (3) to account for the averaging. The combined uncertainty is ±0.18 RD. Since C is defined in terms of unity plus or minus a fractional (as opposed to percentage) uncertainty, the 95% confidence limits on C are 0.9982 and 1.0018.

4.1.3 The B Factor. The purpose of this factor is to account for wide-range transducer output-voltage variations that are independent of the measured pressure. The two sources of such variations are less-than-perfect repeatability in zero-offset measurements and errors in recording of the output voltages fitted against the reference pressures.

For purposes of efficiency and convenience, a worst-case approach will be adopted in calculating limits on B. Appendix C contains pertinent data from the laboratory calibrations most recently performed on the absolute pressure transducers; Table C-1 lists the information from the 32 installed and spare wide-range transducers. The largest pressure-offset standard error will be selected from Table C-1, and this value will be expanded to yield a 95% confidence interval. The interval will then be centered at the pressure offset extremes from Table C-1, so that the two sets of limits will bound offset variations over the entire batch of wide-range LOFT transducers. After conversion from pressures to voltages, these limits will be merged with the voltage-recording uncertainty. The two sets of limits on B will then be ready for insertion into Equation (1).

The largest pressure-offset standard error from Table C-1 is $\pm 1.352 \times 10^{-2}$ MPa (transducer 741166). This value must be multiplied by the appropriate Student's T Table value (two-tailed, $t_{61,0.025} = 2.00$) to create a $\pm 2.70 \times 10^{-2}$-MPa, 95% confidence interval. Table C-1 also shows that transducer 741168 has the largest negative offset (-32.77×10^{-2} MPa), and that transducer 741178 has the largest positive offset (1.49×10^{-2} MPa). Centering the interval at the offset extremes yields -35.54×10^{-2} and -30.07×10^{-2} MPa, and -1.21×10^{-2} and $+4.19 \times 10^{-2}$ MPa.

The MPa-to-voltage conversion factor is yielded by dividing the nominal full-range output voltage (0.030 V) by the nominal full-range pressure (20.69 MPa) with a result of 1.45×10^{-3} V/MPa. After conversion, the two confidence intervals are from -5.15×10^{-4} to -4.36×10^{-4} V and from -1.75×10^{-5} to 6.08×10^{-5} V.

The only task remaining is to incorporate the 0.13-RG DDAPS data recording uncertainty, which is introduced before the pre-LOCE pressure test output voltages are fitted against the reference pressures. Multiplying 0.13% times 0.030 V gives 3.9×10^{-5} V. This uncertainty is incorporated into the above limits by root-sum-squaring. The results, and therefore the two sets of 95% confidence bounds on B, are -5.17×10^{-4} and -4.38×10^{-4} V, and -4.27×10^{-5} and 7.22×10^{-5} V.

4.1.4 The S Factor. The purpose of this factor is to place limits on the variations in wide-range transducer output voltages that are dependent on the system pressure. The only sources of such variations are the random errors causing less-than-perfect transducer repeatability at a given pressure. In actuality, these errors have their origins in such phenomena as signal noise, environmental changes, and round-off and truncation errors; not all of the causes are directly related to the transducer itself. Only rarely is it possible to identify and quantify all of the contributions to random errors, because many of the contributions are quite small.

When measuring the magnitude of the random uncertainty, attempts are made to minimize external influences by using a laboratory environment and particularly stable instrumentation. These laboratory studies have established that the random errors from inherent transducer variability and any residual external influences have a distribution width that varies linearly with the measured pressure.

During INEL laboratory calibrations, the method used to characterize the random uncertainty magnitude is to take several independent data sets over the pressure range. A standard error "e" is calculated for the slope coefficient D_1, and the standard error is then divided by one-hundredth of the D_1 value to yield a percentage of reading (RD) uncertainty "s."

Mathematically, $s = 100\ e/D_1$ and

$$S = 1 \pm \frac{s}{100} = 1 \pm \frac{e}{D_1} = \frac{D_1 \pm e}{D_1}.$$

Since e is a standard error and since 95% confidence bounds on S are necessary, multiplication by Student's T Table value "t" is required.

$$S_{95} = \frac{D_1 \pm te}{D_1} = 1 \pm \frac{ts}{100}.$$

Table C-1 shows that transducer 741166 has the largest (worst-case) RD uncertainty value, 11.00×10^{-2} RD. Multiplication by 2.00, the appropriate Student's T Table value, yields 0.22 RD. Because S is defined on a fractional (as opposed to percentage) basis, the 95% confidence limits on S are $1 \pm 2.2 \times 10^{-3}$, or 0.9978 and 1.0022.

4.1.5 Calibration Uncertainty Summary. The 95% minimum confidence extremes on the factors C, K, S, and B (two sets) have been calculated in the preceding subsections. For purposes of generating worst-case limits on the zero-offset (D_0) uncertainty, all possible combinations of these factor extremes must be used as input to Equation (1). Since the two sets of bounds on B cannot be mixed, a total of two groups of 16 combinations results. The input and output of the 32 calculations are summarized in Table 1.

Recall that finding the largest difference between D_0 values within a group is the objective of this exercise. This maximum difference is the worst-case estimate of the confidence interval on the offsets generated by the least-squares fits against the reference pressures. As shown by Table 1, the maximum difference (0.1279 MPa) is between combinations 21 and 24. Assuming that this interval is symmetric, the zero-offset uncertainty from the wide-range transducer reference calibrations is ±0.064 MPa.

One additional factor must be considered with respect to the offset (independent of pressure) uncertainty from the reference calibration process. The zero-offset value in the LOFT Control Records is not changed unless it differs by at least 0.0345 MPa from the offset generated by the pre-LOCE least-squares regression. Consequently, there is a procedural uncertainty of ±0.0345 MPa. This factor must be combined with the ±0.064-MPa uncertainty inherent in the calibration offset by root-sum-squaring. The net result for high-range transducer offset uncertainty is approximately ±0.073 MPa.

Because Equation (2) contains only factors C and S, the 95% confidence interval for the pressure-dependent uncertainty is easily calculated. The extremes about the nominal scale coefficient (689.54 MPa/V) are 692.30 and 686.78 MPa/V.

$$692.30 - 689.54 \text{ MPa/V} = 689.54 - 686.78 \text{ MPa/V} = 2.76 \text{ MPa/V}.$$

As with the zero offsets, the existing D_1 coefficient is not replaced by the calibration D_1, unless a statistically significant difference exists between the two values. In particular, the Control Records coefficient D_{1CR} is only changed if

$$D_{1CR} - D_{1LS} > s_{LS} \times t_{\nu,\ 0.025}$$

TABLE 1. ZERO-OFFSET EXTREMES SUMMARY

	C	K (MPa)	S	B (V)[a]	D_o (MPa)
1	1.0018	0.128	1.0022	-4.38×10^{-4}	0.4325
2	0.9982	0.128	1.0022	-4.38×10^{-4}	0.4312
3	1.0018	0.080	1.0022	-4.38×10^{-4}	0.3844
4	1.0018	0.128	0.9978	-4.38×10^{-4}	0.4319
5	1.0018	0.128	1.0022	-5.17×10^{-4}	0.4869
6	1.0018	0.128	0.9978	-5.17×10^{-4}	0.4863
7	1.0018	0.080	1.0022	-5.17×10^{-4}	0.4388
8	1.0018	0.080	0.9978	-4.38×10^{-4}	0.3840
9	0.9982	0.128	1.0022	-5.17×10^{-4}	0.4856
10	0.9982	0.128	0.9978	-4.38×10^{-4}	0.4319
11	0.9982	0.080	1.0022	-4.38×10^{-4}	0.3844
12	1.0018	0.080	0.9978	-5.17×10^{-4}	0.4384
13	0.9982	0.128	0.9978	-5.17×10^{-4}	0.4850
14	0.9982	0.080	1.0022	-5.17×10^{-4}	0.4375
15	0.9982	0.080	0.9978	-4.38×10^{-4}	0.3840
16	0.9982	0.080	0.9978	-5.17×10^{-4}	0.3841
17	1.0018	0.128	1.0022	$+7.22 \times 10^{-5}$	0.0799
18	0.9982	0.128	1.0022	$+7.22 \times 10^{-5}$	0.0801
19	1.0018	0.080	1.0022	$+7.22 \times 10^{-5}$	0.0318
20	1.0018	0.128	0.9978	$+7.22 \times 10^{-5}$	0.0793
21	1.0018	0.128	1.0022	-4.27×10^{-5}	0.1593
22	1.0018	0.128	0.9978	-4.27×10^{-5}	0.1587
23	1.0018	0.080	1.0022	-4.27×10^{-5}	0.1111
24	1.0018	0.080	0.9978	$+7.22 \times 10^{-5}$	0.0314
25	0.9982	0.128	1.0022	-4.27×19^{-5}	0.1591
26	0.9982	0.128	0.9978	$+7.22 \times 10^{-5}$	0.0795
27	0.9982	0.080	1.0022	$+7.22 \times 10^{-5}$	0.0319
28	1.0018	0.080	0.9978	-4.27×10^{-5}	0.1108
29	0.9982	0.128	0.9978	-4.27×10^{-5}	0.1586
30	0.9982	0.080	1.0022	-4.27×10^{-5}	0.1110
31	0.9982	0.080	0.9978	$+7.22 \times 10^{-5}$	0.0316
32	0.9982	0.080	0.9978	-4.27×10^{-5}	0.1107

a. Combinations 1-16 were performed with the B confidence interval centered at -0.3277 MPa. Combinations 17-32 were performed with the B confidence interval centered at 0.0149 MPa.

where

D_{1LS} = value generated by the least-squares regression

s_{LS} = the standard error in D_{1LS}

$t_{\nu, 0.025}$ = value obtained from a Student's T Table

ν = the degrees of freedom.

Though s_{LS} and t_{ν} are variables, their product equals one-half the 95% confidence interval on D_{1LS}. The worst-case estimate of this product is the result of the preceding paragraph, 2.76 MPa/V. Thus, an upper bound on the coefficient difference before D_{1CR} would be changed is 2.76 MPa/V. This procedural uncertainty must be combined by root-sum-squaring with the 2.76-MPa/V uncertainty in D_{1LS}. The net uncertainty is 3.90 MPa/V. In order to express this quantity in terms of a percentage of reading, it must be divided by one-hundredth the nominal D_1 value (6.8954 MPa/V). Therefore, the pressure-dependent uncertainty from the reference calibration process is estimated (worst-case) as ±0.57 RD.

4.2 Data Recording Errors

Now that uncertainties have been estimated for the pre-LOCE calibrations, uncertainties must be treated that occur during the LOFT tests themselves. Ambient temperature changes during a test are negligible, and the only remaining sources of uncertainty are data recording errors. The two recording systems, DDAPS and WBFM, have already been described in Section 3.4 for the reference transducers. The uncertainties for the two systems are 0.13 RG (percent of range) for the DDAPS and 1.1 RG for the WBFM. The range of these transducers is 20.69 MPa; therefore, the respective recording uncertainties are $\pm 2.7 \times 10^{-2}$ and ±0.23 MPa. Because these uncertainties are independent of the measured pressure, they must be treated as zero offset uncertainties. Merging the above values with the ±0.073-MPa calibration offset uncertainty by root-sum-squaring yields net offset uncertainties of ±0.077 MPa for DDAPS recording and ±0.24 MPa for WBFM recording.

4.3 Transducer Height Differences

As shown in Figures 4 and 5, most of the wide-range transducers are located on either the primary coolant loop or the blowdown loop. Since the reference transducers, PE-PC-5 and PE-PC-6, are also located on the primary coolant loop, most wide-range transducers are at approximately the same elevation within the LOFT primary system as the reference transducers. However, Figure 3 shows that four wide-range transducers are located within the reactor vessel at varying distances relative to the loop elevation.

The reactor vessel is nominally filled with water to approximately the height of the reference transducers. One would expect the reactor-vessel transducers to yield consistently higher pressures than the reference transducers by an amount equal to ρgh, where ρ is the water density, g is the gravitational constant, and h is the height difference. This is not the case. It is convenient during posttest data evaluations to make direct comparisons of local system dynamics by overlaying pressure transducer plots. To this end, offsets are determined during the pre-LOCE static pressure tests that force the reactor-vessel transducers to agree with the reference transducers at the initiation of a test. In the strict sense of absolute pressure, this process introduces biases into the reactor-vessel data. But, because these biases are of known amount and because they are deliberate, they will not be treated as errors in this document.

The height differences are a source of error during a transient test in several other respects, however. While the elevation differences between the reactor-vessel and reference transducers are obviously fixed, the height of the water column is not. During a large break configuration test, the reactor-vessel water level

drops significantly. Also, the water density is not constant. At the start of a transient test, the coolant "blows down"; that is, water vapor in solution at the high initial pressure rapidly forms bubbles after depressurization. This phenomenon leads to a net density decrease. Moreover, the reactor scrams at the start of a transient. Since power is no longer being generated, the water gradually cools, leading to a density increase.

It is virtually impossible to generalize these sources of bias error into meaningful uncertainties. As shown in Figure 3, the four wide-range reactor vessel transducers are located within different regions with respect to thermal-hydraulic behavior of the coolant. Furthermore, the biases discussed in the preceding paragraph are all time-dependent in a fashion intimately determined by individual test characteristics. Since LOFT tests essentially never repeat themselves in terms of duration and thermal-hydraulic behavior, any analysis from past tests would not necessarily apply to future tests. Rather than attempting to place limits on the above effects for individual reactor-vessel transducers, the reader is simply cautioned that uncertainty values quoted in this report for the wide-range measurements do not account for correctable effects. Should more accurate assessment of reactor-vessel transducer behavior become necessary, actual test data can be used to calculate appropriate correction factors.

4.4 Wide-Range Measurement Summary

Uncertainties applicable to all 32 wide-range transducers have been described and quantified. The offset uncertainty from the combined sources that are independent of the measured pressure is ±0.077 MPa for DDAPS data recording and is ±0.24 MPa for WBFM recording. The pressure-dependent uncertainty is ±0.57 RD.

5. NARROW-RANGE MEASUREMENTS

The uncertainties in the narrow-range (0- to 1.38-MPa) absolute pressure data arise from three distinct sources. These sources are errors in the calibration coefficients, transducer temperature variations, and output-voltage recording errors. The uncertainties from these sources are most conveniently separated as to whether they are independent of or dependent on the measured pressure, and the analysis will proceed on this basis. Following the terminology used previously, the pressure-independent uncertainties will be classified as zero-offset uncertainties.

5.1 Zero-Offset Uncertainties

The narrow-range transducers do not receive a full calibration by multi-pressure comparisons to the reference transducers during pre-LOCE testing. As a result, a least-squares regression process is not performed. Instead, a straightforward comparison is made at only the 1.38-MPa point of the cold pressure test, since the higher pressure points are beyond the range of these transducers. This comparison serves only as an offset calibration.

As with the wide-range transducer pre-LOCE calibrations, this one-point comparison is made against a reference transducer average. Data recording errors before calibration must be considered in a manner similar to that for the wide-range transducers. Also, there is a corresponding minimum threshold before the offset coefficient is changed. All these factors will be evaluated in the calculation of a calibration uncertainty.

Unlike the wide-range transducers, a comparison cannot be made between the narrow-range and reference transducers during the pre-LOCE hot pressure test. Saturation conditions dictate that the system pressure is in excess of 1.38 MPa at the hot pressure test temperature of 555 K. Consequently, there is no opportunity to correct the offset coefficients for ambient temperature increases as the reactor warms in preparation for the hot pressure test and the transient itself. Laboratory calibration data obtained at different temperatures will be used to estimate the uncertainty from this source.

The above factors will account for inaccuracies and inadequacies in the D_0 coefficients for the 10 installed or spare narrow-range transducers. The only remaining pressure-independent sources of error are the data recording systems used during the LOFT tests. These errors will be treated in a manner analogous to that for the reference and wide-range transducers.

5.1.1 Calibration Uncertainty. The first task in calculating the zero-offset calibration uncertainty is to find a worst-case value for the entire batch of narrow-range transducers that essentially represents the lack of repeatability in measurement of the offsets. The best assessment of this effect is given by the D_0 standard errors listed in Table C-2. The largest value found there is $\pm 3.98 \times 10^{-4}$ MPa for transducer 741157. This standard error is converted into a 95% confidence interval by multiplication, using the appropriate two-tailed value from a Student's T Table (2.00, 63 data points). The product is 7.96×10^{-4} MPa.

The next step is to calculate the total uncertainty in the reference transducer average at the cold pressure test point of 1.38 MPa. Per Section 4.1.1, the pressure-independent 95% confidence interval on the averaged reference pressure is $^{+0.020}_{-0.028}$ MPa. Per Section 4.1.2, the pressure-dependent uncertainty in the average is ± 0.18 RD. Taking 0.18% of 1.38 MPa gives 2.49×10^{-3} MPa. The total reference pressure uncertainty is yielded by root-sum-squaring the values. The result is $^{+2.02}_{-2.81} \times 10^{-2}$ MPa.

The narrow-range transducer output voltages are recorded exclusively on the DDAPS during pre-LOCE testing. These voltages are converted into pressures in software before being compared to the reference pressure. The DDAPS recording uncertainty is ± 0.13 RG. Taking 0.13% of 1.38 MPa gives 1.80×10^{-3} MPa.

As in the case of the wide-range transducers, the offset coefficient is not changed unless a 0.0345-MPa minimum difference is found between the reference pressure and that from an individual narrow-range transducer. Thus, there is a $\pm 3.45 \times 10^{-2}$ MPa procedural uncertainty.

The total calibration uncertainty (95% confidence) in the narrow-range transducer zero-offset coefficients is given by root-sum-squaring the uncertainty contribution values of $\pm 7.96 \times 10^{-4}$, $^{+2.02}_{-2.81} \times 10^{-2}$, $\pm 1.80 \times 10^{-3}$, and $\pm 3.45 \times 10^{-2}$ MPa. The net result is $^{+4.0}_{-4.5} \times 10^{-2}$ MPa.

5.1.2 Transducer Temperature Variations. As noted previously, the lack of any opportunity for a hot pressure test calibration causes ambient temperature changes in the neighborhood of the transducer bodies to become a source of uncertainty. The treatment of this uncertainty is patterned after that already performed for the reference transducers in Section 3.2. There, the effects of a 20-K (worst-case) ambient temperature increase were estimated by interpolation between laboratory coefficient values obtained at two different temperatures.

Table C-2 shows that, while all 10 narrow-range transducers received room-temperature (300-K) calibrations, four of the transducers also were calibrated at 343 K. All four high-temperature offset values are more positive than their room-temperature counterparts by amounts ranging from 2.8×10^{-3} to 1.68×10^{-2} MPa. Assuming the 1.68×10^{-2} MPa value is worst-case for all 10 transducers, multiplying by a $\frac{20\ \text{K}}{343\ \text{K} - 300\ \text{K}}$ interpolation factor yields a 7.81×10^{-3}-MPa estimate of the largest positive offset shift induced by the ambient temperature increase. Since only the 300-K values are used in the software conversions, this shift must be treated as an uncertainty in the 300-K offsets. Since the available data indicates that this bias is exclusively in the positive direction, the 7.81×10^{-3} MPa value will only be added to the 4.0×10^{-2}-MPa upper confidence bound from calibration. The approximate result is 4.8×10^{-2} MPa.

The 95% confidence interval on the zero offsets from the combined effects of calibration and temperature variations is $^{+4.8}_{-4.5} \times 10^{-2}$ MPa. Because only symmetric limits are suitable for presentation in the summary table, this interval is conservatively modified to $\pm 4.8 \times 10^{-2}$ MPa.

5.1.3 Data Recording Errors. Now that the D_0 uncertainty has been estimated for the narrow-range transducers, the only remaining pressure-independent sources of uncertainty are the two data recording systems used during the LOFT tests themselves. As described in Section 3.4, the uncertainties are 0.13 RG for the DDAPS and 1.1 RG for the WBFM. Taking 0.13% and 1.1% of 1.38 MPa gives 1.8×10^{-3} and 1.5×10^{-2} MPa, respectively. Merging these values with the $\pm 4.8 \times 10^{-2}$ MPa offset uncertainty yields net pressure-independent uncertainties of $\pm 4.8 \times 10^{-2}$ MPa for DDAPS recording and $\pm 5.0 \times 10^{-2}$ MPa for WBFM recording.

5.2 Pressure-Dependent Uncertainties

Only two pressure-dependent sources of uncertainty exist for the narrow-range measurements. The first source is the inherent variability in the transducers and the associated signal-conditioning electronics. As discussed in Section 4.1.4, this variability is induced by a large number of factors included under the broad heading of random errors. The second source is the difference in ambient temperature between the laboratory calibration and the operating reactor environment. The only significant effects of this temperature difference are shift biases observed in the D_1 slope coefficients.

For reasons stated previously, comparisons cannot be made between the reference pressures and the narrow-range transducers outputs at more than one pressure and temperature. Consequently, the slope coefficients cannot be adjusted during the pre-LOCE pressure tests. The only recourse available for estimating pressure-dependent uncertainties is to use the laboratory calibration data. Because bonded strain-gage transducer characteristics frequently change with use, it should be recognized that the results of this section may not accurately represent current narrow-range transducer behavior.

5.2.1 Transducer Response Variations. Variability in measured transducer response at a given pressure is caused by random errors such as signal noise, truncation errors, etc. Laboratory studies have confirmed that the width of the random error distribution is a linear function of the measured pressure. The method used to characterize the distribution width as a function of pressure is to divide the D_1 standard error by the coefficient value, and then to convert this number into a percentage. This percent of reading uncertainty value is independent of pressure, though the standard error used in the computation includes contributions from the random errors at all of the pressures used in the calibration cycles.

Following the approaches used earlier in this report, the first step is to find the worst-case percentage of reading uncertainty among the 10 narrow-range transducers. Per Table C-2, the largest 300-K RD value is 16.24×10^{-2} percent for transducer 741151. This value is converted into a 95% confidence interval by multiplying by 2.00, the appropriate Student's T Table value. The resulting interval is approximately ±0.33 RD.

5.2.2 Transducer Temperature Variations. As shown by Table C-2, an ambient temperature increase caused shifts in the D_1 coefficients for all four narrow-range transducers calibrated at 343 K. The general objective of this section is to develop a worst-case RD uncertainty value accounting for this effect.

The observed D_1 shifts range from +0.04 to -0.08 MPa/V. Multiplying by 20 K/43 K to account for the maximum measured temperature increase near the reactor (see Section 3.2) reduces this range to approximately +0.02 to -0.04 MPa/V. In order to provide some assurance that the shift range is truly worst-case over all 10 transducers, the limits are increased to ±0.05 MPa/V. Using 48 MPa/V for a typical 300-K slope coefficient leads to an uncertainty of approximately ±0.11 RD.

The uncertainty for the combined effects of response variations and slope coefficient bias is conservatively given by arithmetically adding the 0.33 and 0.11 RD values. The net estimate for the pressure-dependent uncertainties is ±0.44 RD.

5.3 Narrow-Range Measurement Summary

Uncertainties appropriate to all 10 narrow-range transducers have been described and quantitatively estimated. The zero-offset uncertainty from combined pressure-independent sources is $\pm 4.8 \times 10^{-2}$ MPa for DDAPS recording and $\pm 5.0 \times 10^{-2}$ MPa for WBFM recording. The net percentage of reading uncertainty from combined pressure-dependent sources is ±0.44 RD.

Section 4.3 addressed a problem for several of the wide-range transducers that is caused by these transducers being located within the reactor vessel at a lower elevation than the reference transducers. The elevation difference leads to unknown uncertainties in the ρgh factor from water-level and water-density changes over the duration of a LOFT test. As a result, the uncertainty values quoted for the wide-range transducers do not necessarily apply to those in the reactor vessel.

As shown by Figure 3, a comparable situation exists for two of the narrow-range transducers. It should be recognized, however, that the effects discussed in Section 4.3 are much less of a problem for the narrow-range reactor-vessel transducers. In general, the narrow-range transducers are used only to monitor local pressures during the reflood phase of a large-break transient. By the time this phase of a test begins, the coolant temperature has stabilized to a large extent, and the water-density changes are almost insignificant. Of course, coolant-level changes affect the outputs of the reactor-vessel transducers, but monitoring such changes during reflood is one of the primary purposes of these measurements.

It should be noted that the preceding narrow-range measurement material does not address how slope coefficient drift is discovered or handled, since only a zero-offset calibration is performed by comparison to the reference transducers. In practice, narrow-range transducers receive periodic in-place calibrations against variable pressure sources. If the behavior of a given narrow-range transducer is suspect, due either to the in-place check or to comparison against other narrow-range transducers, the transducer is replaced by a spare and sent to the INEL standards laboratory for recalibration.

6. BLOWDOWN-SUPPRESSION-SYSTEM MEASUREMENTS

Like the primary coolant system, the blowdown suppression system has measurements with two different ranges. Most of the Precise Sensor transducers have a range from 0 to 0.69 MPa, but several range between 0 and 3.48 MPa. Unlike the primary coolant system, however, the two classes of suppression-system transducers are calibrated in exactly the same manner. Consequently, all of the suppression-system measurements may be treated in the same section of this report.

As with the previously-analyzed classes of absolute pressure transducers, the suppression-system transducers have uncertainty sources arising from calibration coefficients, ambient temperature variations, and output-voltage recording errors. These uncertainties will be conveniently separated as to their dependence or lack of dependence on the measured pressure. As previously done, the pressure-independent uncertainties will be combined under the general heading of zero-offset uncertainties.

6.1 Zero-Offset Uncertainties

There is no direct connection between the LOFT primary coolant system and the blowdown suppression system until a blowdown valve is opened and water begins to flow from the primary system into the suppression tank at the initiation of the transient. Thus, no means exist for comparing the suppression-system transducers to the reference transducers at multiple pressures during pre-LOCE pressure testing. Zero-offset uncertainties due to measurement difficulties and thermal variations must be estimated from manufacturer's calibration data, since the Precise Sensor transducers did not receive a laboratory calibration upon receipt at the INEL. Because the factory calibrations were performed at a different elevation with respect to sea level than that of the LOFT reactor, the zero offsets must be adjusted analogously to those for the reference transducers. This conversion to local absolute pressure is based on the outputs of other pressure transducers, and is therefore also a source of error. Consideration of the above factors will estimate inaccuracies in the D_0 coefficients for the suppression-system transducers. The only remaining pressure-independent sources of uncertainty are the data recording systems used during the LOFT tests.

6.1.1 Calibration Uncertainties. The zero-offset uncertainty from calibration effectively represents the lack of repeatability in laboratory measurements of offset values. Evaluating this uncertainty for each class of suppression-system transducer is somewhat simpler than for previous cases, since no comparison is made to the reference transducers. Essentially, all that is required is to determine a worst-case standard error for each group of transducers, and then to convert these values into 95% confidence intervals.

Table C-3 contains the manufacturer's calibration data for the 16 installed or spare 0- to 0.69-MPa suppression-system transducers. The largest room-temperature offset standard error found in this table is $\pm 3.3 \times 10^{-4}$ MPa for transducer 3746. This standard error is converted into a 95% confidence interval by multiplying by 2.00, the appropriate Student's T Table value. The result is $\pm 6.6 \times 10^{-4}$ MPa.

The calibration data for the two installed and two spare 0- to 3.48-MPa transducers is presented in Table C-4. The largest room-temperature offset standard error is $\pm 8.3 \times 10^{-4}$ MPa for transducer 3709. This standard error is multiplied by 2.00, and the resulting 95% confidence interval is approximately $\pm 1.7 \times 10^{-3}$ MPa.

6.1.2 Transducer Temperature Variations. The 339-K calibration data in Table C-3 shows D_0 shifts from the 300-K data by varying amounts. The largest positive shift found is 9.94×10^{-3} MPa for transducer 3734, and the largest negative shift found is 3.21×10^{-3} MPa for transducer 3721. Since only symmetric limits are of interest, the D_0 thermal shifts are conservatively assumed to fall within $\pm 1.0 \times 10^{-2}$ MPa. Recalling that only a 20-K ambient temperature increase has been measured near the LOFT reactor (see Section 3.2), while the shift magnitudes discussed above were induced by a 39-K increase, a 20/39 interpolation factor must be applied. This changes the confidence interval on offset thermal shifts for the 16, 0.69-MPa transducers to $\pm 5.1 \times 10^{-3}$ MPa.

Following the procedure outlined above, the largest offset shift found in Table C-4 for the 3.48-MPa suppression-system transducers is 7.14×10^{-3} MPa for transducer 3708. The thermal shifts for all four transducers are conservatively assumed to fall within $\pm 7.2 \times 10^{-3}$ MPa. Application of the 20/39 interpolation factor reduces this confidence interval to $\pm 3.7 \times 10^{-3}$ MPa.

6.1.3 Absolute Pressure Adjustment. The suppression-system transducers are susceptible to offset drifts. Prior to a LOFT test, the blowdown suppression tank is vented to the atmosphere and the transducer amplifiers are zeroed. Since this lowers the suppression-system-transducer output voltages by a constant amount, an adjustment must be made in software for each transducer. The value of the adjustment must be equal to containment pressure. Note that an identical process is performed during the pre-LOCE tests for the reference transducers in Section 3.3. Note also that this offset adjustment is not necessary in the case of the primary-coolant-system transducers, since they are calibrated against the reference transducers.

Ambient containment pressure is determined by averaging the responses of three process pressure transducers. Each response must fall between 0.083 and 0.090 MPa, or the response is discarded. Since no other procedural controls or calibration methods for these three transducers exist, a worst-case offset uncertainty of ± 0.007 MPa must be assumed. This uncertainty value applies equally to the 0.69- and 3.48-MPa suppression-system transducers.

6.1.4 Data Recording Errors. Two data systems, the DDAPS and the WBFM, are used to record transducer output voltages during LOFT tests. The respective uncertainties are 0.13 RG (percent of range) and 1.1 RG. Because these uncertainties are independent of the measured pressure, they must be treated as zero-offset uncertainties. Uncertainties 0.13 and 1.1 RG convert to 9.0×10^{-4} and 7.6×10^{-3} MPa, respectively, for the 0- to 0.69-MPa suppression-system transducers. The corresponding uncertainties for the 0- to 3.48-MPa transducers are 4.6×10^{-3} and 3.9×10^{-2} MPa.

6.2 Pressure-Dependent Uncertainties

There are two pressure-dependent sources of uncertainty for the suppression-system transducers. One is the variability in transducer response caused by the occurrence of random errors in the transducer hardware and in the related signal-conditioning electronics. The second source is the thermal difference between the factory calibration and the operating reactor environment. The first source manifests itself as less-than-perfect repeatability in output signal at a given pressure. The only significant effects of the second source are shifts in the D_1 slope coefficients.

6.2.1 Transducer Response Variations. The random errors causing response variations have a distribution width that is a linear function of the measured pressure. This width is related to the measured pressure by dividing the slope coefficient standard error by the coefficient value. The resulting number, which is constant with respect to pressure, is then converted into a percentage of reading (pressure) uncertainty.

The largest room-temperature RD uncertainty among the 0.69-MPa transducers is obtained from Table C-3. This worst-case value is $\pm 8.49 \times 10^{-2}$ RD for transducer 3746. Because this uncertainty is derived from a standard error, it must be multiplied by the appropriate T Table value for conversion into a 95% confidence interval which results in approximately ± 0.17 RD.

The worst-case room-temperature RD uncertainty for the 3.48-MPa transducers is found in Table C-4 as $\pm 3.58 \times 10^{-2}$ RD for transducer 3709. Multiplying by 2.00 for 95% confidence yields an interval of approximately $\pm 7.2 \times 10^{-2}$ RD.

6.2.2 Transducer Temperature Variations. The 339-K data from Table C-3 shows D_1 slope coefficient shifts from the 300-K values by amounts ranging from -0.15 to +0.06 MPa/V. Following conservative, symmetric-limit approaches used for previous classes of transducers, it is assumed that all D_1 shifts

fall between ±0.15 MPa/V. Because only a 20-K increase above room temperature (300 K) has been measured as the LOFT reactor reaches operating conditions, the ±0.15-MPa/V interval must be multiplied by a 20/39 interpolation factor. This reduces the interval to ±0.08 MPa/V. Dividing this interval by 27 MPa/V, the worst-case D_1, yields an RD uncertainty of approximately ±0.30% for the thermally-induced coefficient shifts.

The largest D_1 shift found in Table C-4 for the 3.48-MPa transducers is 0.42 MPa/V. Conservatively assuming ±0.42-MPa/V shift limits and applying the interpolation factor produces a ±0.22-MPa/V interval. Dividing this interval by a worst-case D_1 value of 178 MPa/V yields an RD uncertainty of ±0.12% for the thermal slope-coefficient shifts.

6.3 Suppression-System Measurement Summary

Uncertainties for both the 0.69- and 3.48-MPa blowdown-suppression-system pressure transducers have been described and quantified. Due to the lack of other available information, most of the uncertainty values were estimated using manufacturer's calibration data. These data provide an accurate assessment of transducer behavior shortly after installation. It must be recognized, however, that strain-gage-device characteristics frequently change after a period of use, and that the uncertainties computed may no longer reflect current transducer performance levels.

The above discussion poses the question of how transducers with excessive drift are processed. As with the narrow-range primary-coolant-system transducers, plots from transducers in similar environments are compared against each other after each LOFT test. Anomalous transducers are replaced by spares and sent to the INEL Standards Laboratory for recalibration.

6.3.1 Zero-Offset Uncertainties. The total zero-offset uncertainty for the 0.69-MPa suppression-system measurements is obtained by combining contributions from all of the pressure-independent sources. Root-sum-squaring the 6.6×10^{-4}-MPa calibration uncertainty and the 7.0×10^{-3}-MPa absolute pressure adjustment uncertainty, and adding the 5.1×10^{-3}-MPa uncertainty from thermally-induced coefficient biases produces an uncertainty in the D_0 coefficients of $\pm 1.22 \times 10^{-2}$ MPa. Merging this value with either $\pm 9.0 \times 10^{-4}$ MPa for DDAPS data recording or $\pm 7.6 \times 10^{-3}$-MPa for WBFM data recording yields approximate zero-offset uncertainties of $\pm 1.3 \times 10^{-2}$ and $\pm 1.5 \times 10^{-2}$ MPa, respectively.

The 3.48-MPa suppression-system measurements have uncertainties of $\pm 1.7 \times 10^{-3}$ MPa from calibration, $\pm 3.7 \times 10^{-3}$ MPa from thermal shifts, and $\pm 7.0 \times 10^{-3}$ MPa from the absolute pressure adjustment. Combining these values yields an approximate uncertainty in the D_0 coefficients of $\pm 1.1 \times 10^{-2}$ MPa. Inclusion of the data recording uncertainties ($\pm 4.6 \times 10^{-3}$ MPa for DDAPS and $\pm 3.9 \times 10^{-2}$ MPa for WBFM) produces approximate total offset uncertainties of $\pm 1.2 \times 10^{-2}$ MPa with DDAPS recording and $\pm 4.1 \times 10^{-2}$ MPa with WBFM recording.

6.3.2 Pressure-Dependent Uncertainties. The total pressure-dependent uncertainty for the 0.69-MPa suppression-system measurements is obtained by arithmetically adding the ±0.17-RD output-response uncertainty to the ±0.30-RD thermal bias uncertainty. The result is approximately ±0.47 RD.

The output-response uncertainty for the 3.48-MPa measurements is $\pm 7.2 \times 10^{-2}$ RD. The thermal bias uncertainty for these transducers is ±0.12 RD. Adding the two intervals yields a total uncertainty of approximately ±0.20 RD.

7. RESPONSE LIMITATIONS

Any measurement system requires a finite amount of time to respond to a transient impulse in the quantity being measured. More specifically, some time is necessary both for the transducer to convert the impulse into an electrical signal and for the associated electronics to amplify, filter, and either display or record the signal. When the transducer is physically separate from the impulse, an additional delay is introduced in transmitting the impulse from the source to the transducer. Within the context of the LOFT absolute pressure measurements, the water-filled standoff tubes, used to mount the primary-coolant-system transducers, cause such additional response delays.

Were only a net time delay to result from the effects of the aforementioned factors, there would be little concern; any significant lags could be removed by compensation in software, if necessary. However, should the transient impulses be complicated in shape or shorter in duration than the overall response time of the measurement system, the measurement data will be distorted to some extent. In fact, the data may provide no indication that the impulses ever occurred.

Data inaccuracies originating in response lags are practically impossible to quantify, since the distortions are intimately determined by characteristics of the individual transient impulses. As a direct consequence, such inaccuracies have traditionally not been considered in calculations of overall measurement uncertainties. Instead, attempts have been made within the LOFT Program to predict the most rapid changes in the quantities of interest, to design the respective measurement systems accordingly, and to prevent the response-derived data deviations wherever possible.

Rise time T_R is defined as the time required by a measurement system, or component thereof, to go from 10 to 90% of the full-scale value of an impressed step function. This is equivalent to 2.2 times the classical time constant for first-order (undamped, nonresonant) systems. Rise times will be estimated in the subsequent portions of this report for the standoff tubes, the five types of absolute pressure transducers, and for the two data recording systems. Results will then be combined for all system component combinations.

7.1 Standoff Tube Delays

As described in Section 2, the absolute pressure transducers for the primary coolant system are separated from the origins of the pressure signals by water-filled standoff (pressure transmission) tubes. While most of the standoffs are completely external to the reactor, Figure 3 illustrates the fact that most of the lengths of the reactor-vessel standoffs are enclosed within the vessel. These standoffs are at considerably higher temperatures than the external standoffs, which are approximately at ambient air temperature. Over the temperature range of interest, the sound (pressure signal) velocity in water decreases significantly with increasing temperature. The delay or lag time for transmitting a signal from the source to the transducer is obtained by dividing the standoff length by the sound velocity. Because the reactor-vessel standoffs are subject to higher temperatures and correspondingly slower sound velocities and because these standoffs have generally longer lengths, these standoffs form the limiting case with respect to delay time calculations.

The reactor-vessel standoff lengths are given by Table 2 (top four rows); the longest tube length is 10.405 m. A worst-case (though realistic) sound velocity within the vessel of 802 m/s is obtained from 600-K, 15-MPa conditions. Since temperature gradient information for the portion of this standoff outside the vessel is not available, the 802 m/s value is assumed valid over the entire length. Division of the length by the velocity yields a 1.3×10^{-2} s worst-case delay time for all of the standoffs.

TABLE 2. MEASURED AND CALCULATED RESONANT FREQUENCIES FOR THE TRANSDUCER STANDOFF TUBES ON THE PRIMARY COOLANT SYSTEM

Pressure Measurements	Standoff Tubing Lengths (m)	Measured Frequencies (Hz)	Calculated[a] Frequencies (Hz)
PE-1ST-1A, -1B	10.405	20, 50, 62, 140	22[b]
PE-1ST-3A, -3B	5.544	33, 60	42[b]
PE-2ST-1A, -1B	9.754	20, 33	24[b]
PE-1UP-1A, -1A1	5.537	--[c]	42[b]
PE-PC-1	1.029	380	374
PE-PC-2	1.029	400	374
PE-PC-4	10.655	30, 120, 480	36
PE-PC-5	2.438	--[c]	158
PE-PC-6	2.438	--[c]	158
PE-BL-1	1.029	350	374
PE-BL-2	1.029	420	374
PE-BL-3	0.622	700	620
PE-BL-4	1.118	325	345
PE-BL-6	0.597	790	645
PE-BL-8	0.610	780	632

a. Sound velocity (1541 m/s) at pressure of 8.9 MPa and temperature of 320 K.

b. Sound velocity (931 m/s) at pressure of 6.9 MPa and temperature of 555 K for reactor-vessel standoffs.

c. Not installed at the time of the power-spectral-density measurements.

7.2 Standoff Tube Resonances

The effects of the standoffs are not confined to causing delays that increase the net response time of the measurement system. Each of these tubes has a fundamental resonant frequency f yielded by

$$f = \frac{0.25\ v}{l} \text{ (one end open)} \qquad (4)$$

where v is the speed of sound in water and l is the length of the tube. Of course, v is dependent on the temperature and pressure of the water.

Resonant tube frequencies were measured during subcooled blowdown thermal-hydraulic testing, before the LOFT reactor attained criticality, by obtaining power spectral densities from those transducers installed at the time. The results of these measurements are presented in Table 2. Frequencies were calculated according to Equation (4) at pressure and temperature conditions approximately equivalent to those during the testing; the calculated values are also provided by Table 2. The measured and calculated values are in generally good agreement, especially in light of the fact that the temperature gradients over the length of each tube cannot be accurately approximated by a single temperature.

Different sound velocities were used in the frequency calculations for the reactor vessel and for the rest of the primary coolant system. Most of each reactor-vessel standoff length was at a temperature of 555 K within the vessel during the testing; the other standoffs were approximately at the ambient air temperature of 320 K. At 6.9 MPa, the test system pressure, the speed of sound in water is 931 m/s at 555 K and is 1541 m/s at 320 K.

The power spectral density for the PE-PC-4 standoff is supplied by Figure 9. As shown by this figure and by Table 2, frequencies in addition to the fundamental resonances were measured on certain of the transducer standoffs. Observed frequencies significantly above the fundamental frequencies are caused by valves, tee's, and elbows acting as wave reflection surfaces. (The frequency content below 20 Hz on Figure 9 is not of interest in transient response analysis.) Each section of tubing between such surfaces resonates according to Equation (4) and essentially behaves as a separate standoff with reduced resonance amplitude.

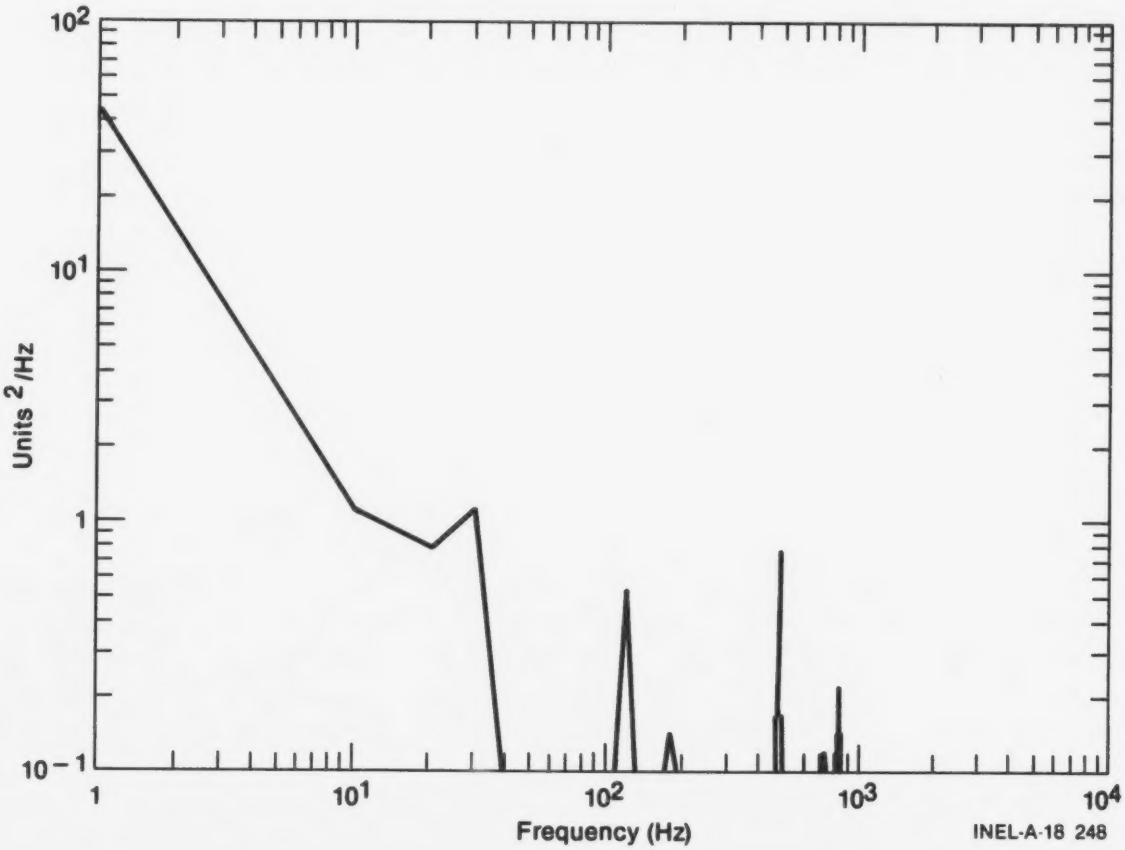

Figure 9. Power spectral density for PE-PC-4 during the Test L1-3A subcooled blowdown.

Were pressure data to be recorded at frequencies including the fundamental and other resonant frequencies, the data would necessarily be distorted. Frequency components of the pressure pulses matching the resonances would be magnified out of proportion to their original amplitudes, and the recorded shapes and magnitudes of the pressure pulses would be altered. When data accuracy is of primary importance, the resonant frequencies must be removed by low-pass electronic filtering. Per Table 2, frequencies down to and including 20 Hz must be eliminated.

The resonant frequencies cannot be removed without some cost in terms of frequency response, since electronic filters also have response times. As noted in Section 2.3, a response-versus-accuracy choice was made in the design of the two recording systems—the analog WBFM system being selected for fast transient response and the digital DDAPS system for accuracy. A 10-Hz low-pass filter is installed on the DDAPS for large-break transients, and a 1-Hz filter is utilized for small-break tests. (Small-break transients are slow in terms of pressure changes and long in terms of duration. A 1-Hz filter is employed to facilitate recording of data over long periods, rather than to further eliminate resonant frequencies.) The WBFM has a 3-kHz internal low-pass filter; because it has proven inadequate for reducing high-frequency noise, an additional 1-kHz filter is now used.

The response or rise time T_R (10 to 90%) of a single-stage, resistance-capacitance filter is given by

$$T_R = 0.35/F_C \qquad (5)$$

where F_C is the cutoff (-3-dB) frequency. Insertion of 1, 10, and 1000 Hz into Equation (5) yields response times for the data systems of 0.35 s (DDAPS, small break), 3.5×10^{-2} s (DDAPS, large break), and 3.5×10^{-4} s (WBFM).

7.3 Transducer Response

The absolute pressure transducers require some time to convert pressure pulses into electrical signals. The exact amount of time necessary is intimately dependent on the method of construction; generally, the fewer mechanical parts required by the conversion, the faster the response.

A reasonable estimate of transducer response times may be obtained by treating the absolute pressure transducers as single-stage electronic filters. The natural frequencies are given in Appendix A as 44 kHz for the wide-range Teledyne Taber transducers, 7 kHz for the narrow-range Teledyne Taber transducers, 500 Hz for the Precise Sensors transducers, and 12 kHz for the Bell and Howell reference transducers. Insertion of these frequencies into Equation (5) yields respective response times of 8×10^{-6}, 5×10^{-5}, 7×10^{-4}, and 3×10^{-5} s.

7.4 Data System Response

The data system response times are given in Reference (3) as 1.8×10^{-5} s for the WBFM and 3.5×10^{-2} s for the DDAPS. The primary difference between the two systems with regard to response is the analog-to-digital converter in the DDAPS.

7.5 Response Limitation Summary

The response delays introduced by the various measurement system components may not simply be added to generate net response times. For example, by the time a transducer output has risen to the equivalent of 90% of the magnitude of a pressure pulse, the low-pass filter may have risen to 50% and the recording system to 20%. Thus, the response times for the pressure-to-voltage conversion, the filtering, and the recording are most legitimately combined by root-sum-squaring. However, little can happen on the standoff (primary-coolant-system) measurements until the pressure pulse is transmitted through the tube; this transmission time must be combined by straightforward addition.

Combining the response times per the above guidelines yields the measurement system values shown on Table 3 for the various component combinations. These values illustrate the fact that response variations between transducer types are insignificant. Only the lack of standoffs for the Precise Sensors transducers, mounted on the blowdown suppression system, makes a difference.

TABLE 3. ABSOLUTE PRESSURE MEASUREMENT SYSTEM RESPONSE TIMES
(values in seconds)

Transducer Type	DDAPS, Small Break	DDAPS, Large Break	WBFM
Wide-Range Teledyne Taber	0.365	6.25×10^{-2}	1.34×10^{-2}
Narrow-Range Teledyne Taber	0.365	6.25×10^{-2}	1.34×10^{-2}
Precise Sensors (no standoffs)	0.352	4.97×10^{-2}	7.83×10^{-4}
Bell and Howell	0.365	6.25×10^{-2}	1.34×10^{-2}

8. CONCLUSIONS

Measurement uncertainties and response times have been estimated in the preceding sections for the five types of absolute pressure measurements obtained from the LOFT reactor. The results of the estimating calculations are summarized in this section. Comparisons are also made between these estimates and the requirements listed in Reference 1 and Reference 2.

8.1 Measurement Accuracy

LOFT absolute pressure measurements are accurate within the 95% confidence-level uncertainty estimates on Table 4. Uncertainty values are presented in this table for each general source of uncertainty as well as for total offset and pressure-dependent uncertainties. A net uncertainty is calculated at a given pressure for any of the five transducer types by first multiplying the pressure (in MPa) by the total pressure-dependent percent of reading (RD) uncertainty value, then dividing the result by 100, and by finally adding the divided value to the total zero-offset uncertainty. Equivalently, the net uncertainty U at a pressure P is given by

$$U\ (95\%\ \text{confidence}) = \pm \left(B + \frac{P \cdot RD}{100} \right)$$

where B is the bias (zero-offset) uncertainty and where RD is the pressure-dependent uncertainty.

Reference 1 lists a requirement of one percent of range for the primary-coolant-system measurements, and does not address the blowdown suppression system. This limit converts to ±172.4 kPa for the 17.24-MPa reference transducers, to ±206.9 kPa for the wide-range transducers, and to ±13.8 kPa for the narrow-range transducers. Examination of Table 4 reveals that the reference and wide-range measurements meet this requirement when the data are recorded on the DDAPS, but not when recorded on the WBFM. The narrow-range measurements exceed the accuracy limit on both recording systems.

Reference 2 contains accuracy requirements of ±(90 kPa + 5 RD) for the primary coolant system and ±(1.8 kPa + 5 RD) for the blowdown suppression system. Per Table 4, the Bell and Howell reference transducers meet the primary-coolant-system requirement for DDAPS recording over the entire presssure range and for WBFM recording above 2.3 MPa. Similarly, the wide-range Teledyne Taber transducers pass the requirement throughout their range on the DDAPS and pass above 3.4 MPa on the WBFM. The narrow-range instruments meet the Reference 2 limits on both recording systems. The 0.69-MPa Precise Sensors transducers pass the blowdown-suppression-system accuracy requirement above 0.25 MPa on the DDAPS and above 0.29 MPa on the WBFM. The 3.48-MPa instruments are sufficiently accurate with respect to Reference 2 above 0.22 MPa on the DDAPS and above 0.82 MPa on the WBFM.

8.2 Measurement Response

Response times for the absolute pressure measurements were estimated in Section 7. The results for measurements on the primary coolant system, as condensed from Table 3, are 0.365 s for DDAPS recording during a small-break transient, 6.25×10^{-2} s for DDAPS recording during a large-break test, and 1.34×10^{-2} s for WBFM recording. Measurements made by the transducers flush-mounted (no standoffs) on the blowdown suppression system are more rapid; these response times are 0.352 s for small-break DDAPS recording, 4.97×10^{-2} s for large-break DDAPS recording, and 7.83×10^{-4} s for WBFM recording.

TABLE 4. SUMMARY OF ABSOLUTE PRESSURE MEASUREMENT UNCERTAINTIES (95% confidence)

	Primary Coolant System[a]			Blowdown Suppression System	
	Reference[b] (17.24 MPa)	Wide Range (20.69 MPa)	Narrow Range (1.38 MPa)	0.69 MPa	3.48 MPa
Zero Offset (MPa)					
Calibration[c]	$\pm 1.6 \times 10^{-2}$	$\pm 7.3 \times 10^{-2}$	$^{+4.0}_{-4.5} \times 10^{-2}$	$\pm 6.6 \times 10^{-4}$	$\pm 1.7 \times 10^{-3}$
Thermal Bias	2.1×10^{-2}	--[d]	8.0×10^{-3}	$\pm 5.1 \times 10^{-3}$	$\pm 3.7 \times 10^{-3}$
Absolute Pressure Adjustment	$\pm 7.0 \times 10^{-3}$	--[d]	--[d]	$\pm 7.0 \times 10^{-3}$	$\pm 7.0 \times 10^{-3}$
Data Recording					
Digital	$\pm 2.2 \times 10^{-2}$	$\pm 2.7 \times 10^{-2}$	$\pm 1.8 \times 10^{-3}$	$\pm 9.0 \times 10^{-4}$	$\pm 4.6 \times 10^{-3}$
WBFM	± 0.19	± 0.23	$\pm 1.5 \times 10^{-2}$	$\pm 7.6 \times 10^{-3}$	$\pm 3.9 \times 10^{-2}$
Total[e]					
Digital	$\pm 4.3 \times 10^{-2}$	$\pm 7.7 \times 10^{-2}$	$\pm 4.8 \times 10^{-2}$	$\pm 1.3 \times 10^{-2}$	$\pm 1.2 \times 10^{-2}$
WBFM	± 0.20	± 0.24	$\pm 5.0 \times 10^{-2}$	$\pm 1.5 \times 10^{-2}$	$\pm 4.1 \times 10^{-2}$
Pressure Dependent (RD)					
Calibration[c]	± 0.20	± 0.57	± 0.33	± 0.17	$\pm 7.2 \times 10^{-2}$
Thermal Bias	± 0.11	--[d]	± 0.11	± 0.30	± 0.12
Total	± 0.30	± 0.57	± 0.44	± 0.47	± 0.20

a. Does not include special considerations of reactor-vessel transducers.

b. Where a difference between PE-PC-5 and -6 exists, only the larger value is reported.

c. Includes considerations of repeatability, traceability, and nonlinearity.

d. Included within the calibration uncertainty.

e. Values from calibration, setting to absolute pressure, and data recording are root-sum-squared. The thermal bias value is arithmetically summed.

The Reference 1 primary-coolant-system response requirement of 0.5 s is met in all cases with ample margin. (Reference 1 does not address the blowdown suppression system.) Reference 2 contains response requirements for the primary coolant system of 0.03 s during subcooled blowdowns and 0.85 s during saturated blowdowns. Per the above estimated response times, which are independent of the type of blowdown, Reference 2 requirements are met for both recording systems during saturated transient phases and on the WBFM during both transient phases. The response limit of 0.03 s is exceeded for DDAPS recording during subcooled blowdowns. Reference 2 also has a limit of 0.15 s for blowdown-suppression-system pressure measurements. This requirement is met for WBFM recording and for large-break DDAPS recording, but is exceeded for DDAPS recording during a small-break transient.

8.3 Measurement Performance Overview

The comparisons between the estimated accuracy and response performance levels and the respective requirements can be summarized quite briefly. The absolute pressure measurements meet the accuracy limits for DDAPS recording and exceed these limits to some extent for WBFM recording; the pressure measurements meet the response limits for WBFM recording and exceed these limits to some extent for DDAPS recording. (The blowdown suppression-system transducers exceed the Reference 2 accuracy limit at low pressures due to a very restrictive ±1.8-kPa bias uncertainty limit.) It follows directly that the recording systems (including low-pass filters), rather than the pressure transducers, are the limiting factors in overall measurement system performance. State-of-the-art recording technology does not permit combining the accuracy of digitization with the rapidity of analog recording. For this reason, as well as for recording redundancy, the LOFT Program has elected to record critical pressure measurements in parallel on one digital and one analog system.

9. REFERENCES

1. System Design Description 1.4.1D, *Test Assembly Experimental Measurements System, LOFT Integral Test System*, July 1980.

2. John D. Burtt, *LOFT Measurement Requirements Document*, NUREG/CR-0246, TREE-1197, July 1978.

3. P. A. Quinn, *LOFT Data Acquisition and Visual Display System (DAVDS) Uncertainty Analysis*, Supplement 1 to LOFT Technical Report 141-39, November 1975.

4. C. M. Nightengale et al., *LOFT Nonnuclear Data Reduction and Qualification Manual*, LOFT Technical Report 141-63, May 1979.

BLANK PAGE

APPENDIX A

PRESSURE TRANSDUCER PERFORMANCE SPECIFICATIONS

BLANK PAGE

APPENDIX A

PRESSURE TRANSDUCER PERFORMANCE SPECIFICATIONS

The following listing summarizes the specification requirements used to procure the LOFT absolute pressure transducers over a period of approximately six years. In general, the requirements follow product literature on instruments commercially available at the times of the purchasing actions. Since technological advancements were made during the six-year period, requirements were modified and manufacturers changed in order to take advantages of any improvements. Some variation in individual requirements was dictated by differences in application; for example, use of the Bell and Howell transducers as references for the primary coolant system necessitates a small error band.

For convenience in use of the subsequent list, the following key categorizes the transducers by pressure range, manufacturer, and area of installation.

A. 0 to 20.69 MPa; Teledyne Taber; primary coolant system

B. 0 to 1.38 MPa; Teledyne Taber; primary coolant system

C. 0 to 3.48 MPa; Precise Sensors Inc., blowdown suppression system

D. 0 to 0.69 MPa; Precise Sensors Inc., blowdown suppression system

E. 0 to 17.24 MPa; Bell and Howell CEC Div., primary coolant system

1. Excitation voltage: 10 VDC (A, B, C, D, E).

2. Full-scale output: 30 mV (A, B, E); 20 mV (C, D).

3. Resolution: infinite (A, B, C, D, E).

4. Bridge resistance: 350 ohms (A, B, C, D, E).

5. Minimum insulation resistance (measured between any terminal and the case): 10^9 ohms at 50 VDC (A, B, C, D); 5×10^8 ohms at 45 Vd-c (E).

6. Overload pressure (minimum pressure to which transducer may be subjected with no shift of output characteristics upon subsequent usage): 31.04 MPa (A); 20.69 MPa (B); 4.12 MPa (C); 0.83 MPa (D); 34.48 MPa (E).

7. Burst pressure (minimum pressure to which transducer may be subjected without incurring leakage or other mechanical damage): 31.04 MPa (A); 27.52 MPa (B); 17.40 MPa (C); 3.45 MPa (D); 51.72 MPa (E).

8. Minimum operating life (at full-scale pressure): 10^4 hours (A, B, C, D, E).

9. Compensated temperature range: 300-360 K (A, B); 278-395 K (C, D); 220-395 K (E).

10. Error band (combined repeatability, linearity, and hysteresis): ±0.5% of full scale (A, B, C, D); ±0.25% of full scale (E).

11. Zero balance (over the compensated temperature range): within ±2% of full scale (A, B, C, D, E).

12. Vibration error (per 9.8 m/s^2 of acceleration along any orthogonal axis): ±0.002% of full scale (A, B); ±0.1% of full scale (C, D); ±0.003% of full scale (E).

13. Thermal zero shift (over the compensated temperature range): ±0.018% of full scale/K (A, B); ±0.009% of full scale/K (C, D, E).

14. Thermal sensitivity shift (over the compensated temperature range): ±0.009%/K (A, B, C, D, E).

15. Natural frequencies: 44 kHz (A), 7 kHz (B), 500 Hz (C, D), 12kHz (E).

APPENDIX B

UNCERTAINTY PROPAGATION THROUGH CALIBRATION REGRESSIONS

BLANK PAGE

APPENDIX B

UNCERTAINTY PROPAGATION THROUGH CALIBRATION REGRESSIONS

The slope coefficient D_1 and the zero offset D_0 for each wide-range (0- to 20.69-MPa) primary-coolant-system pressure transducer are determined during the pre-LOCE pressure tests. The coefficient values are placed in the LOFT Control Records, and they are later used in software to calculate pressures from transducer output voltages recorded during each LOFT test.

The coefficient values are calculated during the pre-LOCE tests by least-squares regressions of individual transducer output voltages (x-axis) versus reference pressures (y-axis). The reference pressures are averages of the pressures obtained from reference transducers PE-PC-5 and PE-PC-6; the pressure values are nominally 1.38, 3.45, 6.90, 10.34, 13.79, and 15.52 MPa. Thus, the wide-range transducers receive a six-point calibration against the reference transducers.

The reference pressures possess errors associated with ambient temperature variations, calibration uncertainties, and voltage-recording uncertainties. Errors are also present in the measurement and recording of the individual output voltages fitted against the reference pressures. These errors propagate through the regression process, and create uncertainties in the wide-range transducer calibration coefficients and in the pressures later calculated from the coefficients.

1. DERIVATION OF FORMULAS

The purpose of this appendix is to derive general formulas whereby wide-range transducer coefficient uncertainties may be estimated after input of representative values for source errors. In accordance with the convention used throughout this document, it is assumed that all errors may be bounded either by offset uncertainties or by percentage of reading (RD) uncertainties. In general, the errors contributing to zero-offset uncertainties are constant biases that are too small or too troublesome to be removed in a calibration sequence. Contributions to the RD uncertainties are typically from random errors having a distribution width that increases linearly with the pressure being measured.

Let

r_i = the calculated reference pressures (averages of the pressures generated from the reference transducer coefficients and from the output voltages measured at the six target system pressures),

y_i = the nominal, target reference pressures (1.38 MPa, 3.45 MPa, etc.),

c_i = the RD uncertainty in each r_i (fixed percentage of y_i),

K = the constant offset (sum of small biases) in each r_i,

x_i = the nominal wide-range transducer output voltages at the six target system pressures,

v_i = the actual wide-range transducer output voltages,

s_i = the RD uncertainty in each v_i (fixed percentage of x_i),

and

B = the constant offset (sum of small biases) in each v_i.

(While K and B are constants in actuality, the constant values can only be estimated within limits. The estimate extremes for these constants will not be symmetric about zero.)

The least-squares-fitting process generates a line $y = D_1 x + D_o$ for each transducer from the points (v_i, r_i), $i = 1,\ldots, 6$. Define the fitting function $f(D_1, D_o)$ such that

$$f(D_1, D_o) = \sum_{i=1}^{6} \left(D_1 v_i + D_o - r_i\right)^2.$$

Minimizing f establishes the line that best fits the six points. The fitting function is minimized by finding a D_1 and a D_o such that $\frac{\partial f}{\partial D_o} = 0$ and such that $\frac{\partial f}{\partial D_1} = 0$. These criteria yield the following simultaneous equations.

$$\sum_{i=1}^{6} r_i = 6 D_o + D_1 \sum_{i=1}^{6} v_i \qquad \text{(B-1)}$$

$$\sum_{i=1}^{6} r_i v_i = D_o \sum_{i=1}^{6} v_i + D_1 \sum_{i=1}^{6} v_i^2 \qquad \text{(B-2)}$$

(For simplicity, $\sum_{i=1}^{6}$ will hereafter be represented by $\sum$.)

The solutions to the simultaneous equations are

$$D_o = \frac{1}{\Delta}\begin{vmatrix} \sum r_i & \sum v_i \\ \sum r_i v_i & \sum v_i^2 \end{vmatrix} = \frac{1}{\Delta}\left(\sum v_i^2 \sum r_i - \sum v_i \sum r_i v_i\right) \qquad \text{(B-3)}$$

and

$$D_1 = \frac{1}{\Delta}\begin{vmatrix} 6 & \sum r_i \\ \sum v_i & \sum r_i v_i \end{vmatrix} = \frac{1}{\Delta}\left(6 \sum r_i v_i - \sum v_i \sum r_i\right), \qquad \text{(B-4)}$$

where

$$\Delta = \begin{vmatrix} 6 & \sum v_i \\ \sum v_i & \sum v_i^2 \end{vmatrix} = 6 \sum v_i^2 - \left(\sum v_i^2\right). \qquad \text{(B-5)}$$

While the above equations are valid, they are useless from the standpoint of estimating uncertainties. Further manipulation is required in order to separate the r_i and v_i factors into their nominal and off-nominal components. Restating the variable definitions in mathematical form,

$$y_i + K - \frac{c_i\, y_i}{100} \leq r_i \leq y_i + K + \frac{c_i\, y_i}{100}$$

and

$$x_i + B - \frac{s_i\, x_i}{100} \leq v_i \leq x_i + B + \frac{s_i\, x_i}{100}.$$

The fact that c_i and s_i are constant percentages of y_i and x_i, respectively, allows some simplification. Define bivalued factors C and S such that

$$C = 1 \pm \frac{c_i}{100} \text{ and } S = 1 \pm \frac{s_i}{100}.$$

Thus, r_i is bounded by $Cy_i + K$ and v_i is bounded by $Sx_i + B$. Note that C and S are defined on the basis of unity plus or minus a fractional (as opposed to a percentage) uncertainty.

Again, the equations being developed must express D_0 and D_1 in terms of nominal values and factors accounting for off-nominal deviations. These equations will be used in the main text to calculate extremal values for D_0 and D_1 and, thereby, to generate worst-case D_0 and D_1 uncertainties. Since only worst-case deviations from nominal are of interest, r_i and v_i may be set equal to their limits. Thus,

$$r_i = Cy_i + K \tag{B-6}$$

and

$$v_i = Sx_i + B. \tag{B-7}$$

Substituting Equations (B-6) and (B-7) into (B-3), (B-4), and (B-5),

$$D_o = \frac{1}{\Delta}\left\{CS^2\left(\sum x_i^2 \sum y_i - \sum x_i \sum x_i y_i\right) + KS^2\left[6\sum x_i^2 - \left(\sum x_i\right)^2\right] + BCS\left(\sum x_i \sum y_i - 6\sum x_i y_i\right)\right\}, \tag{B-8}$$

$$D_1 = \frac{1}{\Delta} CS\left(6\sum x_i y_i - \sum x_i \sum y_i\right), \tag{B-9}$$

and

$$\Delta = S^2\left[6\sum x_i^2 - \left(\sum x_i\right)^2\right]. \tag{B-10}$$

2. INPUT OF NOMINAL VALUES

Equations (B-8), (B-9), and (B-10) have been derived in a form using nominal values and constants accounting for deviations from these values. The y_i are target pressures at which various pre-LOCE tests are procedurally performed. The values are 1.38, 3.45, 6.90, 10.34, 13.79, and 15.52 MPa. The x_i are fractions of full-range output voltages at these reference pressures. All of the wide-range transducers have a nominal 0.030-V output (10 V excitation) at their upper limit of 20.69 MPa. Each x_i is yielded by dividing the i-th reference pressure by 20.69 MPa and by then multiplying the result by 30 mV. Thus, x_1 equals 2 mV, x_2 equals 5 mV, x_3 equals 10 mV, x_4 equals 15 mV, x_5 equals 20 mV, and x_6 equals 22.5 mV.

Knowing the x_i and y_i values allows the summation quantities in Equations (B-8), (B-9), and (B-10) to be evaluated. The results are

$$D_o = CS\ (1.467 \times 10^{-3}\ MPa) + KS\ (1.000) - BC\ (689.54\ MPa/V) \qquad \text{(B-11)}$$

and

$$D_1 = C/S\ (689.54\ MPa/V). \qquad \text{(B-12)}$$

Note that C and S are dimensionless, while B has units of volts and K is in megapascals.

APPENDIX C

CALIBRATION RESULTS FOR THE ABSOLUTE PRESSURE TRANSDUCERS

BLANK PAGE

APPENDIX C

CALIBRATION RESULTS FOR THE ABSOLUTE PRESSURE TRANSDUCERS

Five groups of absolute pressure transducers, purchased from three different manufacturers, are analyzed in this report. These groups are the wide- and narrow-range Teledyne Taber primary-coolant-system transducers, the 0.69- and 3.48-MPa Precise Sensors blowdown-suppression-system transducers, and the Bell and Howell reference transducers.

Laboratory calibration results, based on 63 data points from each transducer, are used in the main text to determine worst-case values for a group and to estimate the effects of ambient temperature increases. Tables C-1 and C-2 contain INEL standards laboratory results from the wide- and narrow-range Teledyne transducers, respectively. Since several Teledyne transducers have been recalibrated after a period of use, only the most recent results are presented. The suppression-system transducers were not calibrated upon receipt at the INEL; instead, manufacturer's calibration results are used. Thus, Tables C-3 and C-4 (the 0.69- and 3.48-MPa Precise Sensor transducer results, respectively) contain no recent information. Only two Bell and Howell reference transducers have been purchased to date. Rather than tabulating the calibration results here, the reference transducer information is presented in Section 3 of the main text.

TABLE C-1. CALIBRATION RESULTS FOR THE WIDE-RANGE TRANSDUCERS

Serial Number	D_o (10^{-2} MPa)	D_o Standard Error (10^{-3} MPa)	D_1 (MPa/V)	D_1 Standard Error (10^{-2} MPa/V)	Percent of Reading Uncertainty (10^{-2}%)
741161	-6.03	8.79	690.12	49.38	7.16
741162	-6.00	8.34	691.14	46.90	6.79
741163	-5.98	8.48	692.86	47.59	6.86
741164	-4.38	6.55	693.04	3.66	0.53
741165	-4.93	7.31	689.63	41.38	6.00
741166	-4.10	13.52	695.80	76.55	11.00
741167	-5.26	7.72	689.69	43.45	6.30
741168	-32.77	8.76	689.40	48.97	6.00
741169	-32.60	7.70	686.70	44.33	6.46
741170	-5.29	7.83	690.13	44.00	6.38
741171	-5.13	7.51	690.32	42.18	6.11
741172	-5.10	7.37	693.97	41.66	6.00
741173	-5.26	7.62	690.40	42.82	6.20
741174	-6.10	8.82	690.53	49.59	7.18
741175	-4.89	7.23	691.29	40.69	5.89
741176	-5.59	7.92	694.45	44.76	6.45
741177	-5.29	7.69	691.59	43.31	6.26
741178	+1.49	7.30	694.80	43.55	6.27
741179	-5.36	7.70	688.62	43.17	6.27
741180	-5.23	7.64	689.93	42.90	6.22
741182	-5.99	8.49	691.96	47.79	6.91
741183	-4.39	6.73	691.38	37.92	5.49
741184	-4.71	6.96	689.96	39.10	5.67
761739	-2.30	6.41	693.06	36.55	5.27
761740	+1.15	6.69	692.90	37.93	5.47
761741	-4.55	6.83	692.15	38.62	5.58
761742	-5.12	6.97	691.21	39.31	5.69
761743	-4.77	6.88	690.35	38.62	5.59
762059	-11.45	10.14	692.79	56.88	8.21
762061	-6.03	8.21	689.75	48.97	7.10
772540	-11.59	5.86	609.45	28.97	4.75
772542	-24.70	6.15	607.01	30.00	4.94

TABLE C-2. CALIBRATION RESULTS FOR THE NARROW-RANGE TRANSDUCERS

Serial Number[a]	D_o (10^{-2} MPa)	D_o Standard Error (10^{-4} MPa)	D_1 (MPa/V)	D_1 Standard Error (10^{-2} MPa/V)	Percent of Reading Uncertainty (10^{-2} %)
741151	-4.20×10^{-2}	1.32	49.08	7.97	16.24
	-3.92×10^{-2}	1.38	49.03	8.30	16.93
741152	1.06×10^{-3}	2.14	47.91	1.24	2.59
741153	7.26×10^{-2}	1.12	49.55	0.77	1.55
	8.89×10^{-2}	1.45	49.47	1.01	2.04
741154	5.66×10^{-4}	2.06	50.39	1.24	2.46
741155	1.88×10^{-3}	2.07	47.35	1.17	2.48
741156	8.25×10^{-2}	1.79	49.09	1.23	2.51
	9.93×10^{-2}	1.66	49.13	1.31	2.67
741157	3.97×10^{-3}	3.98	50.08	2.41	4.81
741158	-6.90×10^{-6}	1.10	47.16	0.65	1.32
741159	7.66×10^{-2}	1.29	47.48	0.86	1.81
	8.92×10^{-2}	0.74	47.42	0.50	1.05
741160	1.88×10^{-4}	1.66	49.14	1.03	2.10

a. For transducers with two rows of data, the top row of data were obtained at 300 K and the bottom row at 343 K. For transducers with a single row of data, the data were obtained at 300 K.

TABLE C-3. CALIBRATION RESULTS FOR THE 0.69-MPa TRANSDUCERS

Serial Number[a]	D_o (10^{-3} MPa)	D_o Standard Error (10^{-4} MPa)	D_1 (MPa/V)	D_1 Standard Error (10^{-2} MPa/V)	Percent of Reading Uncertainty (10^{-2} %)
3720	-1.33	3.08	28.94	2.28	7.88
	-2.92	3.67	28.87	2.69	9.32
3721	-3.41	2.35	35.18	2.14	6.08
	-6.62	2.92	35.12	2.62	7.46
3722	-2.18	2.76	32.77	2.34	7.14
	-4.76	3.60	32.70	2.97	9.08
3727	6.39	2.61	31.29	2.14	6.84
	4.33	3.23	31.23	2.62	8.39
3728	2.27	1.66	32.52	1.38	4.24
	1.81	2.15	32.45	1.79	5.52
3729	-0.27	1.48	35.78	1.38	3.86
	0.16	1.79	35.71	1.66	4.65
3730	-0.57	2.70	36.21	2.48	6.85
	0.37	2.81	36.06	2.62	7.27
3733	-6.59	2.62	36.28	2.41	6.64
	3.22	3.03	36.30	2.83	7.80
3734	-5.98	1.69	36.08	1.59	4.41
	3.96	1.79	36.06	1.66	4.60
3735	-8.86	3.07	32.41	2.48	7.65
	-5.62	3.23	32.47	2.69	8.28
3736	-3.43	2.09	34.34	1.86	5.42
	0.36	1.94	34.38	1.72	5.00
3741	2.13	1.69	32.48	1.45	4.46
	4.64	2.54	32.46	2.21	6.81
3742	2.48	2.21	31.14	1.79	5.75
	1.26	2.98	31.13	2.41	7.74
3743	-8.79	2.23	31.05	1.72	5.54
	-8.74	3.01	31.04	2.34	7.54

TABLE C-3. (continued)

Serial Number[a]	D_o (10^{-3} MPa)	D_o Standard Error (10^{-4} MPa)	D_1 (MPa/V)	D_1 Standard Error (10^{-2} MPa/V)	Percent of Reading Uncertainty (10^{-2} %)
3744	-1.42	2.86	32.31	2.34	7.24
	-1.98	3.60	32.26	2.97	9.21
3746	1.61	3.30	27.08	2.30	8.49
	2.03	3.78	26.98	2.63	9.75

a. Top row of data for each transducer was obtained at 300 K; the bottom row was obtained at 339 K.

TABLE C-4. CALIBRATION RESULTS FOR THE 3.48-MPa TRANSDUCERS

Serial Number[a]	D_o (10^{-4} MPa)	D_o Standard Error (10^{-4} MPa)	D_1 (MPa/V)	D_1 Standard Error (10^{-2} MPa/V)	Percent of Reading Uncertainty (10^{-2} %)
3706	-4.28×10^{-2}	6.40	201.68	5.45	2.70
	-3.34×10^{-2}	6.07	201.35	5.17	2.57
3707	2.97×10^{-2}	7.50	178.43	5.79	3.24
	2.86×10^{-2}	8.31	178.01	6.41	3.60
3708	-4.80×10^{-3}	7.83	194.40	6.48	3.33
	2.34×10^{-3}	10.40	194.07	8.62	4.44
3709	2.45×10^{-3}	8.31	184.97	6.62	3.58
	5.98×10^{-3}	9.73	184.63	7.72	4.18

a. Top row of data for each transducer was obtained at 300 K; the bottom row was obtained at 339 K.